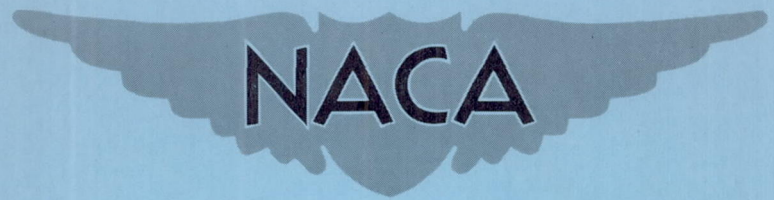★ CASE FILE COPY

RM L50H09

NACA

RESEARCH MEMORANDUM

MEASUREMENTS OF AERODYNAMIC CHARACTERISTICS OF A

35° SWEPTBACK NACA 65-009 AIRFOIL MODEL WITH $\frac{1}{4}$-CHORD

FLAP HAVING A 31-PERCENT-FLAP-CHORD OVERHANG

BALANCE BY THE NACA WING-FLOW METHOD

By Harold I. Johnson and Harold R. Goodman

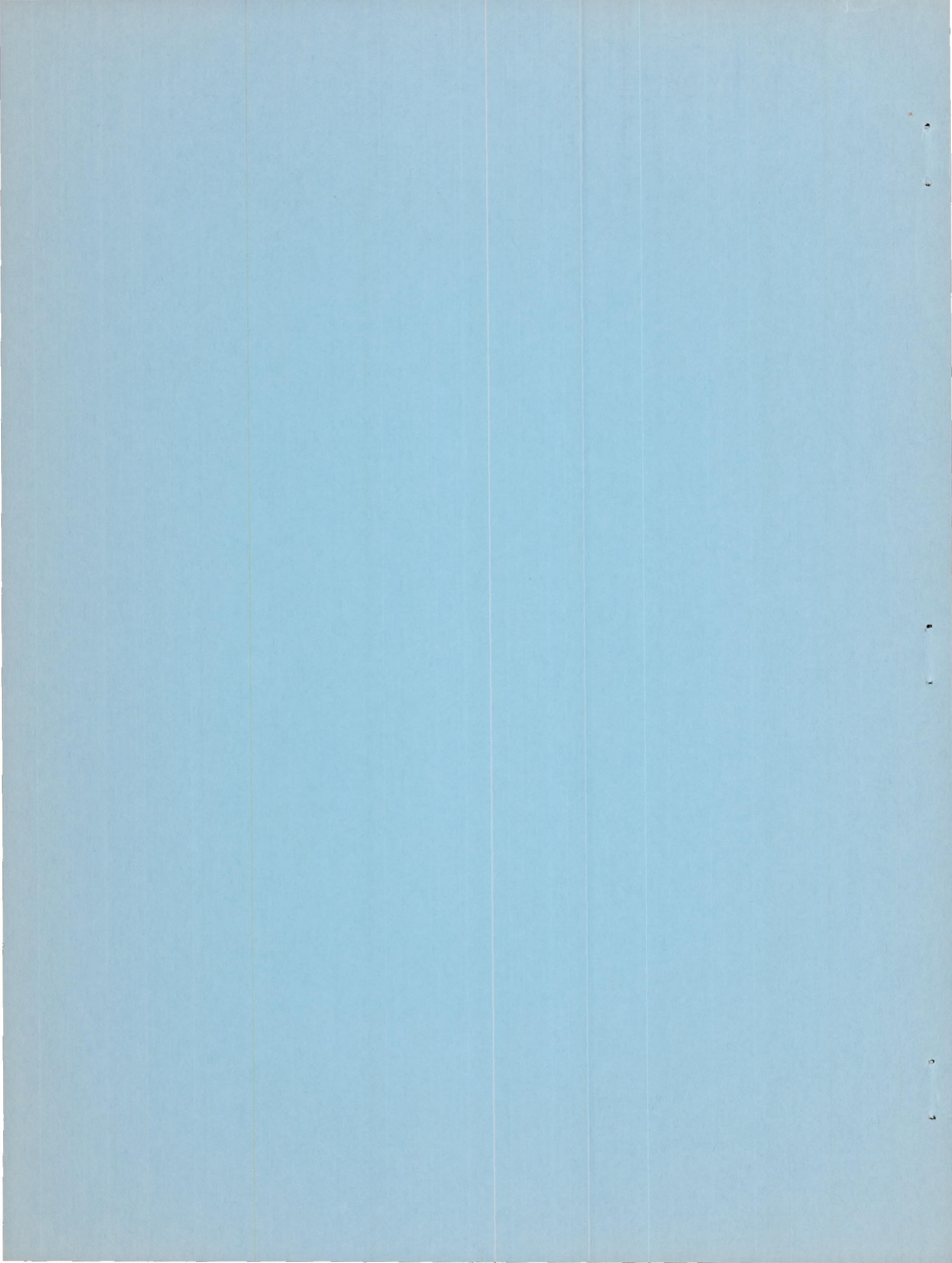Langley Aeronautical Laboratory
Langley Air Force Base, Va.

NATIONAL ADVISORY COMMITTEE
FOR AERONAUTICS

WASHINGTON

September 25, 1950
Declassified August 23, 1954

NATIONAL ADVISORY COMMITTEE FOR AERONAUTICS

RESEARCH MEMORANDUM

MEASUREMENTS OF AERODYNAMIC CHARACTERISTICS OF A

35° SWEPTBACK NACA 65-009 AIRFOIL MODEL WITH $\frac{1}{4}$-CHORD

FLAP HAVING A 31-PERCENT-FLAP-CHORD OVERHANG

BALANCE BY THE NACA WING-FLOW METHOD

By Harold I. Johnson and Harold R. Goodman

SUMMARY

An untapered 35° sweptback airfoil-flap model, representative of either a wing or a tail surface, has been fitted with several $\frac{1}{4}$-chord full-span flaps differing only in type of aerodynamic balance. A plain flap, a horn-balanced flap, and a beveled-trailing-edge flap have already been tested and the subject investigation was made with a flap that had a 31-percent-flap-chord overhang balance. Some of the more important results are as follows:

The general trends of the aerodynamic parameters with Mach number were similar to those previously measured with other types of flaps on the model. The overhang-balanced flap was slightly more effective in producing lift than a comparable plain flap below a Mach number of 1.05. Between Mach numbers of 1.05 and 1.17, the converse was true. The overhang balance tested was relatively ineffective in reducing the hinge-moment variation with either angle of attack or flap deflection. Below a Mach number of 0.90, the hinge moment due to flap deflection was reduced approximately 30 percent by use of the overhang balance, but the hinge moment due to angle of attack was sensibly unaffected. Between Mach numbers of 0.90 and 1.00, the overhang balance lost its effectiveness and at Mach numbers between 1.00 and 1.15, there was no clearcut difference between the hinge-moment characteristics of the overhang-balanced flap and those of a comparable plain flap.

INTRODUCTION

A wing-flow investigation has been made to obtain the hinge-moment and effectiveness characteristics in the transonic speed range of trailing-edge controls incorporating various important types of subsonic aerodynamic balance. In these tests, an untapered 35° sweptback airfoil-flap combination, representative of either a wing or a tail surface, was fitted with $\frac{1}{4}$-chord full-span flaps which differed solely in type of aerodynamic balance. As an adjunct to flap-characteristics data, measurements of model lift and pitching moment with flap fixed were also obtained. The characteristics of a plain flap representing zero aerodynamic balance were reported in reference 1. The characteristics of a horn-balanced flap were reported in reference 2. The characteristics of a beveled-trailing-edge flap and trim tab were reported in reference 3. The data presented herein are from tests of an overhang-balanced flap.

The tests consisted of measurements of the lift, pitching moments, and hinge moments acting on a semispan airfoil-flap model having a sweepback angle of 35°, an aspect ratio of 3.06, a taper ratio of 1.0, an NACA 65-009 section in planes perpendicular to the leading edge, and a full-span true-contour $\frac{1}{4}$-chord flap having an overhang balance of 31 percent of the flap chord. Data were obtained over an angle-of-attack range of -5° to 30°, a flap-deflection range of -18° to 20°, a Mach number range of 0.55 to 1.17, and a Reynolds number range of about 500,000 to 1,400,000. Inasmuch as the tests were made at two widely separated altitude ranges, Reynolds number effects could be investigated; however, the highest Reynolds number encountered was small in comparison with probable full-scale Reynolds numbers.

SYMBOLS

M average Mach number over model

M_A airplane free-stream Mach number

q_A airplane free-stream dynamic pressure

q average dynamic pressure over model

S_A airplane wing area

S total model area (semispan-wing area)

C_{L_A} airplane lift coefficient $\left(\dfrac{\text{Airplane lift}}{q_A S_A}\right)$

C_L model lift coefficient $\left(\dfrac{\text{Model lift}}{qS}\right)$

b   model span normal to wind direction

c   model chord in streamwise direction

$\overline{c}$ model mean aerodynamic chord

C_m model pitching-moment coefficient (measured about axis 17.8 percent M.A.C. ahead of leading edge of M.A.C.) $\left(\dfrac{\text{Model pitching moment}}{qS\overline{c}}\right)$

b_f model flap span along hinge line of semispan model wing

$\overline{c}_f$ flap root-mean-square chord perpendicular to hinge line

C_h model hinge-moment coefficient $\left(\dfrac{\text{Model hinge moment}}{q b_f \overline{c}_f{}^2}\right)$

α angle of attack; angle between model chord plane and direction of relative wind

δ flap deflection; angle between flap chord line and airfoil chord line measured in plane perpendicular to hinge line

C_{L_α} variation of model lift coefficient with angle of attack, per degree $\left(\dfrac{\partial C_L}{\partial \alpha}\right)$

C_{L_δ} variation of model lift coefficient with flap deflection, per degree $\left(\dfrac{\partial C_L}{\partial \delta}\right)$

C_{m_α} variation of model pitching-moment coefficient with angle of attack, per degree $\left(\dfrac{\partial C_m}{\partial \alpha}\right)$

C_{m_δ} variation of model pitching-moment coefficient with flap deflection, per degree $\left(\dfrac{\partial C_m}{\partial \delta}\right)$

C_{h_α} variation of flap hinge-moment coefficient with model angle of attack, per degree $\left(\dfrac{\partial C_h}{\partial \alpha}\right)$

C_{h_δ} variation of flap hinge-moment coefficient with flap deflection, per degree $\left(\dfrac{\partial C_h}{\partial \delta_f}\right)$

$\dfrac{\partial \alpha}{\partial \delta}$ flap relative effectiveness $\left(\dfrac{\partial C_L / \partial \delta_f}{\partial C_L / \partial \alpha}\right)$

Λ sweepback angle

λ taper ratio

A aspect ratio

c_f flap chord in streamwise direction

S_f flap area rear of hinge line

c_b overhang-balance chord perpendicular to hinge line

$\emptyset$ included trailing-edge angle of flap in plane perpendicular to hinge line

APPARATUS

The model was mounted on the upper surface of an F-51D airplane wing as described in reference 1. The variation of the local velocity near the wing surface at the model location is shown in figure 1 and the vertical local velocity gradient at the model location is presented in figure 2. Both gradients were measured with the model removed. Model force and moment coefficients were based on an average dynamic pressure corresponding to an average Mach number over the model area. As indicated by figure 2, the effect of the F-51D wing boundary layer on the velocity distribution over the model was neglected. This proce- dure is considered justifiable because the thickness of the boundary layer as determined from other investigations was of the same order of magnitude as the distance from the F-51D wing surface to the top of the model end plate. Model flexibility effects are small and were neglected. Reference 1 contains a somewhat more detailed discussion of these effects.

A photograph of the model with end plate is shown as figure 3. The model was machined from solid duralumin and the thin circular end plate,

having a diameter equal to the model chord, was fastened to the model root to simulate semispan tests. The flap tang passed through a $\frac{1}{2}$-inch-diameter hole in the end plate. The gap at the leading edge of the flap was equal to 0.013 inch $(0.004\bar{c})$ and was left unsealed for all tests. The chord of the overhang balance was constant and equal to 31 percent of the flap chord rearward of the hinge line. A detail drawing of the model including a list of geometric characteristics is presented in figure 4. A description of the recording instrumentation may be found in reference 2.

TESTS

The data presented herein were obtained from two flights. In the first flight, the model was fixed at zero angle of attack relative to the airplane X-axis and continuous data were recorded as the flap was oscillated through a deflection range of about $\pm 20^\circ$. In the second flight, the flap was fixed at 0° and continuous data were recorded as the model was oscillated through an angle-of-attack range of about -5° to 30°. The model oscillation period was about 1 second and the flap oscillation period was about 0.6 second. By using these rates of oscillation, data were obtained continuously throughout the deflection and angle-of-attack ranges at substantially constant Mach number without introducing any measurable aerodynamic lag except at angles of attack in the region of the stall $(\alpha \gtrsim 15^\circ)$.

Each flight consisted of two test runs, referred to hereinafter as the "high dive" run and the "level flight" run. The high-dive run was made by diving the airplane from 28,000 feet from an indicated airspeed of 220 miles per hour to an airplane Mach number of 0.73 at approximately 18,000 feet. During this run usable data were obtained for an average Mach number range over the model of 0.65 to 1.17 at relatively lower Reynolds numbers. The level-flight run was made by gradually slowing the airplane from an indicated airspeed of 450 miles per hour to 300 miles per hour at an altitude of 5,000 feet following the pull-out of a dive from 15,000 feet altitude. During this run, usable data were obtained for average Mach numbers over the model ranging from 0.55 to 0.95 at comparatively higher Reynolds numbers. Typical variations of Reynolds number with Mach number for the two types of test runs are given in figure 5.

ACCURACY

The accuracy of the major variables in this investigation was estimated to be within the following limits:

Mach number . . . . ±0.01
Angle of attack, degrees . . . . ±0.3
Flap angle, degrees . . . . ±0.3
Lift coefficient . . . . ±0.03
Pitching-moment coefficient . . . . ±0.015
Hinge-moment coefficient . . . . ±0.003

Accuracies of the last three variables listed are given for the lowest test speed; at the highest test speed, these accuracies should be approximately four times better. A large part of the loss in accuracy was attributable to shifts in instrument zeros that occurred gradually during a flight. Hence, the errors in the data appear for the most part as errors in angles of zero lift, angles of zero pitching moment, and angles of zero hinge moment. Because the data at any given Mach number were obtained within a very short period of time (of the order of 1 second), the slopes of the various force- and moment-coefficient curves should be accurate to a degree approaching the instrument capabilities, which, in the present case, add up to about 2 percent of the force and moment ranges measured at intermediate test speeds.

PRESENTATION OF DATA

All force and moment coefficients are presented in accordance with standard NACA conventions regarding definitions and signs. Pitching moments were measured about an axis located 17.8 percent of the mean aerodynamic chord ahead of the leading edge of the mean aerodynamic chord.

Two typical plots of basic data consisting of test points evaluated at one Mach number from the continuous records of force, moments, and position are presented in figure 6. These plots are included to illustrate the nature of the data and the number of test points evaluated at each Mach number inasmuch as the main body of basic data is presented without showing test points in the interest of clarity and brevity. As illustrated in figure 6(a), a small amount of aerodynamic hysteresis was sometimes found at angles of attack in the region of the stall. Where this hysteresis occurred, the data were always faired according to the test points measured during the increasing angle-of-attack portion of the oscillation. The hinge-moment data showed a perceptible amount of hysteresis that was approximately constant at all angles of

attack and flap deflections. This hysteresis resulted from improper electrical damping of the strain-gage circuit used to record hinge moment; however, any error resulting from such hysteresis tends to be eliminated by the procedure used of fairing the data obtained from a complete oscillation.

The following table gives the order of treatment of the basic data as well as a key to the figures:

Figure

Lift:

C_L against $\alpha(\delta = 0^o)$ 7
$C_{L_{max}}$ attained against M 8
C_L against $\delta(\alpha \approx 0^o)$ 9

Pitching moment:

C_m against $\alpha(\delta = 0^o)$ 10
C_m against $\delta(\alpha \approx 0^o)$ 11

Hinge moment:

C_h against $\alpha(\delta = 0^o)$ 12
C_h against $\delta(\alpha \approx 0^o)$ 13

The following table gives the order of treatment of the summary data as well as a key to the figures:

Figure

Lift:

C_{L_α}, C_{L_δ}, $\frac{d\alpha}{d\delta}$ against M 14

Pitching moment:

C_{m_α}, C_{m_δ}, aerodynamic center, center of pressure due to δ
against M 15

Hinge moment:

C_{h_α} against $M(\alpha = 0^o, \delta = 0^o)$ 16
C_{h_δ} against $M(\alpha \approx 0^o, \delta = 0^o)$ 16

DISCUSSION OF BASIC DATA

Lift Characteristics

Lift due to angle of attack.- The variation of lift coefficient
with angle of attack for a flap deflection of 0° for both the high-dive
and level-flight runs is presented in figure 7.

The lift-curve slope at $\alpha = 0^{\circ}$ was substantially unaffected by
Mach number. An increase in lift-curve slope with increasing angle of
attack was present at subsonic Mach numbers as was noted in reference 2.

Within the test angle-of-attack range $(-5^{\circ}$ to $30^{\circ})$ maximum lift or
a value of lift close to maximum lift was obtained. In figure 8, the
variation of the maximum lift coefficients attained over the test angle-
of-attack range is plotted against Mach number. The curve shows a
slight decrease in maximum lift from a Mach number of $M = 0.55$ to
$M = 0.75$ followed by a rapid increase in maximum lift coefficient with
increasing Mach number in the transonic speed range. These data are in
good agreement with the trend obtained from similar less-complete data
presented in reference 1.

Reynolds number had little effect upon either the shape of the lift
curves or the maximum lift coefficients attained.

Lift due to flap deflection.- The variation of lift coefficient
with flap deflection for $\alpha \approx 0^{\circ}$ for both the high-dive and level-
flight runs is presented in figure 9.

The data indicate the flap produced lift effectively throughout the
Mach number and deflection ranges tested. At speeds below $M = 0.95$,
there was some evidence of decreasing flap effectiveness at flap angles
greater than 15°. At Mach numbers of 0.95 and 1.00, the flap effective-
ness was slightly less at small deflections than at large deflections.
At Mach numbers of 1.05 to 1.17, the variation of lift with flap deflec-
tion tended to be linear over the entire range of flap angles covered.
The effects of Reynolds number on the flap effectiveness appear to be
very small - of the order of magnitude of possible experimental error.

Pitching-Moment Characteristics

Pitching moment due to angle of attack.- The variations of
pitching-moment coefficient with angle of attack for a flap deflection
of 0° are shown in figure 10. Pitching moments were measured about an
axis located 17.8 percent of the mean aerodynamic chord ahead of the
leading edge of the mean aerodynamic chord. Because the pitching

moments were measured about an axis well forward of the model aero-
dynamic center, the curves indicate primarily the variation of lift
coefficient with angle of attack rather than any small variations in
aerodynamic-center position.

The data of figure 10 indicate the airfoil developed measurable
amounts of pitching moment at zero angle of attack in spite of having a
symmetrical section. This result is believed to be caused by local
flow curvatures along the model chord. In any application of the data
to a symmetrical section, of course, the data should be interpreted to
give zero lift, pitching moment, and hinge moment at zero angles of
attack and flap deflection. For this purpose, it is suggested the
curves be shifted vertically rather than along the angle-of-attack or
flap-deflection axes.

Pitching moment due to flap deflection.- The variations of the
pitching-moment coefficient with flap deflection for $\alpha \approx 0^\circ$ are
presented in figure 11, and these data show the same general trends as
the lift-coefficient variation with flap deflection.

Hinge-Moment Characteristics

Hinge moment due to angle of attack.- Figure 12 shows the varia-
tions of hinge-moment coefficient with angle of attack for zero flap
deflection. Throughout the angle-of-attack range and at all Mach num-
bers (except above stall at M = 0.95), the slopes of the hinge-moment
curves were negative; this characteristic indicates a tendency of the
flap to float with the relative wind. In the low angle-of-attack range
at Mach numbers below 0.95, the slope of the curves is moderate and then
steepens with increase in the angle of attack. With an increase in Mach
number to supersonic values, the slopes of the hinge-moment curves
become strongly negative at all angles of attack. This trend is charac-
teristic of conventional trailing-edge controls, and it indicates that
the predictions of simple theory for the unswept wing apply qualitatively
to this case also.

The over-all shapes of the hinge-moment curves were not materially
affected by Reynolds number; however, the curves were somewhat less
steep near zero angle of attack for the higher Reynolds number level-
flight data, which indicates an increasing degree of balance with
increasing Reynolds number.

Hinge moment due to flap deflection.- The variations of hinge-
moment coefficient with flap deflection at $\alpha \approx 0^\circ$ are presented in
figure 13. Below a Mach number of 0.90, the flap showed approximately
uniform balancing for flap deflections up to about ±8°. Above a Mach
number of 0.90, the hinge moment due to flap deflection increased

rapidly with increasing Mach number up to a Mach number of 1.05, the
increase indicating a loss in balance. At supersonic Mach numbers the
flap showed approximately uniform balance for deflections up to $\pm 6^\circ$.
At these Mach numbers the hinge-moment curves were steepest at small
deflections, whereas at subsonic speeds the converse was true. The
main effect of increasing Reynolds number was to extend slightly the
flap-deflection range for uniform balancing at subsonic speeds.

DISCUSSION OF SUMMARY DATA

Lift Characteristics

Lift-curve slope.- The variation with Mach number of C_{L_α} measured
at $\alpha = 0^\circ$ is presented in figure 14. The data are in good agreement
with the lift-curve slopes for both the horn-balanced-flap model of
reference 2 and the beveled-trailing-edge-flap model of reference 3.
For the plan form tested, the lift-curve slope was relatively unaffected
by compressibility throughout the Mach number range investigated.
Reynolds number had no consistent measurable effect upon the lift-curve
slope.

Flap effectiveness.- The absolute flap effectiveness C_{L_δ} measured
at $\delta = 0^\circ$ and $\alpha \approx 0^\circ$ is plotted against Mach number in figure 14.
For purposes of comparison, previously unpublished data obtained recently
from tests of a three-hinge plain-flap model are also presented. The
two-hinge plain-flap data of reference 1 were not used for comparison
purposes because some differences were found between the results for
the plain flaps having two and three hinges. These differences were
ascribed to different effects of aeroelastic distortion, particularly
in bending, of the flaps because of the different hinge configurations.
It may be stated, however, that these differences were generally small,
and any major conclusions drawn from the original two-hinge plain-flap
tests would apply also to the results obtained from the three-hinge
plain-flap tests. The data in figure 14 show that the overhang-balanced
flap lost absolute effectiveness $\left(C_{L_\delta} \text{ decreased}\right)$ with increase in
Mach number from $M = 0.55$ to $M = 1.0$. The effectiveness then became
substantially invariant with further increase in Mach number to a Mach
number of 1.17. The overhang-balanced flap was slightly more effective
than the plain flap below a Mach number of 1.05. With further increase
in Mach number the absolute effectiveness of the plain flap was slightly
higher. The lift effectiveness of the overhang-balanced flap was
unaffected by change in Reynolds number within the range tested.

The variation of the relative flap effectiveness $\partial\alpha/\partial\delta$ with Mach
number is also shown in figure 14. The curve shows a continuing loss

in effectiveness with increasing Mach number to a Mach number of 1.0, followed by approximately constant relative effectiveness at higher Mach numbers. The curve is similar in shape to the relative-flap-effectiveness curves of references 1 and 2, but the magnitude of the relative effectiveness was somewhat greater for the overhang-balanced flap than for either the plain flap or the horn-balanced flap. The beveled-trailing-edge flap of reference 3 had slightly greater relative effectiveness at supersonic speeds but also had less at subsonic speeds than the overhang-balanced flap.

Pitching-Moment Characteristics

Pitching-moment coefficient per degree angle of attack.- The pitching-moment slope C_{m_α}, measured at $\alpha \approx 0^o$ and $\delta = 0^o$, is plotted against Mach number in figure 15. The pitching-moment slope was constant to a Mach number of 0.70. With further increase in speed the slope increased to a Mach number of about 1.075 and then reduced slightly in value. Reynolds number effects were negligible.

Pitching moment per degree flap deflection.- The variation of C_{m_δ} with Mach number, measured at $\alpha \approx 0^o$ and $\delta = 0^o$, is also shown in figure 15. The pitching moment per degree flap angle did not change with Mach number to a Mach number of 0.90. The variation with Mach number which occurred at Mach numbers above 0.9 was due primarily to the variation in lift per degree flap deflection rather than to change in the location of the center of pressure. Reynolds number had no measurable effect upon the slopes of the curves.

Aerodynamic-center location.- The positions of the aerodynamic center obtained at $\alpha \approx 0^o$ and $\delta = 0^o$ are plotted against Mach number in figure 15. With an increase in Mach number from 0.55 to 0.70, the aerodynamic center moved forward from 20 percent to 16 percent mean aerodynamic chord. In this connection, the Weissinger theory predicts a low-speed aerodynamic-center position of 20 percent mean aerodynamic chord for the plan form tested. With a further increase in Mach number, there is a gradual rearward movement in aerodynamic-center location to 31 percent mean aerodynamic chord at a Mach number of 1.05. The aerodynamic-center position is then essentially invariant with Mach number from a Mach number of 1.05 to a Mach number of 1.15. Reynolds number had no measurable effect on the aerodynamic-center position.

Center of pressure due to flap deflection.- The position of the center of pressure of lift due to flap deflection obtained at $\alpha \approx 0^o$ and $\delta = 0^o$ is plotted against Mach number in figure 15. There was a fairly steady rearward movement of the center of pressure of lift due to flap deflection over the test Mach number range, a movement from

60 percent mean aerodynamic chord to 96 percent mean aerodynamic chord
for a variation in Mach number from M = 0.55 to M = 1.15.

Hinge-Moment Characteristics

Flap floating tendency Ch_α.- The rate of change of hinge moment
with angle of attack for $\alpha \sim 0^o$ and $\delta = 0^o$ is plotted against Mach
number in figure 16. The overhang-balanced flap had a moderate negative
floating tendency below M = 0.85. With an increase in Mach number
from M = 0.85, the negative floating tendency (tendency to float with
the relative wind) increased to a maximum and was very large at a Mach
number of 1.05. With a further increase in Mach number to the highest
test Mach number the negative floating tendency decreased slightly.
The effect of Reynolds number is evident; increasing Reynolds number in
the subsonic Mach number range reduced the negative floating tendency
of the flap appreciably. Also presented for purposes of comparison are
previously unpublished data from the tests of the three-hinge plain-
flap model with geometric characteristics similar to the overhang-
balanced-flap model but with a flap gap of 0.015 inch. These data show
that, below a Mach number of 0.85, and in the higher Reynolds number
range of the level-flight run, the plain flap had less tendency to float
with the relative wind than the overhang-balanced flap. However, for
the same Mach number range at the lower Reynolds numbers of the high-
dive runs, the plain flap and the overhang-balanced flap had similar
negative floating tendencies. Within the Mach number range of M = 0.85
to M = 1.0, the plain flap exhibited a large variation of flap floating
tendency because the basic hinge-moment curves were very nonlinear. The
basic hinge-moment curves for the overhang-balanced flap were more
nearly linear so that the slopes showed a relatively more gradual
increase in the transonic speed range. Above a Mach number of 1.05,
the plain flap again exhibited less negative floating tendency than the
overhang-balanced flap. On the basis of these results, therefore, it
appears that the overhang balance tested is ineffective for reducing
the hinge moment due to angle of attack on untapered wings of small
sweepback.

Flap restoring tendency Ch_δ.- The rate of change of hinge-moment
coefficient with flap deflection at $\alpha \approx 0^o$ and $\delta = 0^o$ is plotted
against Mach number in figure 16. In addition to the overhang-balanced-
flap data there are also presented data from the previously unpublished
tests of a dimensionally similar three-hinge plain-flap model. A com-
parison of these data shows that below a Mach number of 0.90 and over
the Reynolds number range covered, the overhang balance reduced the
hinge moments due to deflection approximately 30 percent. Above a Mach
number of 0.90, the overhang balance rapidly lost effectiveness to the
extent that, at a Mach number of 1.0 the plain flap had less unbalanced

hinge moment than the overhang-balanced flap. At low supersonic speeds
there was no practical difference between the hinge moments of the
plain flap and the overhang-balanced flap. The rapid loss in
aerodynamic-balance effectiveness of the overhang-balanced flap at
Mach numbers above M = 0.9 and the large hinge moments above M = 1.0
indicate the overhang balance is ineffective in the transonic and low-
supersonic speed range. However, because the 31-percent-flap-chord
overhang balance tested was relatively ineffective even at subsonic
speeds, the possibility exists that a flap having a greater overhang
might exhibit better hinge-moment characteristics throughout the
entire Mach number range investigated.

CONCLUSIONS

On the basis of wing-flow tests of a full-span $\frac{1}{4}$-chord flap having
a 31-percent-flap-chord overhang balance mounted on a 35° sweptback
untapered NACA 65-009 airfoil model of aspect ratio 3.06, the
following conclusions were reached:

1. The general variations in lift, pitching-moment, and hinge-
moment characteristics with Mach number were approximately the same as
those measured previously with plain, horn-balanced, and beveled-
trailing-edge flaps mounted on the model. Within the range tested,
Reynolds number had no measurable effect on lift or pitching-moment
characteristics; however, increasing the Reynolds number by a factor
of about 2 increased the aerodynamic-balance effectiveness noticeably
at small angles of attack and tended to increase the angular ranges
for maximum balance at a given Mach number.

2. The overhang-balanced flap was slightly more effective in
producing lift than a comparable plain flap at Mach numbers below 1.05.
Between Mach numbers of 1.05 and 1.17, the converse was true.

3. The overhang-balanced flap tested appeared to be completely
ineffective in reducing the negative hinge moment due to angle of
attack; at subsonic speeds the hinge moments of the overhang-balanced
flap were slightly greater than those measured on an equivalent plain
flap.

4. The 31-percent-flap-chord overhang balance reduced the hinge-
moment variation with flap deflection about 30 percent at Mach numbers
below 0.90. Between Mach numbers of 0.90 and 1.00 the overhang balance
apparently lost all its effectiveness, and at Mach numbers above 1.00
there was no appreciable difference between the hinge moments of the
overhang-balanced flap and those of an equivalent plain flap.

5. The overhang-balanced flap tested showed no promise as an effective aerodynamic balance at transonic or supersonic speeds; however, because the degree of subsonic balance was low, perhaps further attention should be given to similar flaps having larger overhangs than 31 percent of the flap chord.

Langley Aeronautical Laboratory
    National Advisory Committee for Aeronautics
        Langley Air Force Base, Va.

<div align="center">REFERENCES</div>

1. Johnson, Harold I.: Measurements of Aerodynamic Characteristics of a 35° Sweptback NACA 65-009 Airfoil Model with $\frac{1}{4}$-Chord Plain Flap by the NACA Wing-Flow Method. NACA RM L7F13, 1947.

2. Johnson, Harold I., and Brown, B. Porter: Measurements of Aerodynamic Characteristics of a 35° Sweptback NACA 65-009 Airfoil Model with $\frac{1}{4}$-Chord Horn-Balanced Flap by the NACA Wing-Flow Method. NACA RM L9B23a, 1949.

3. Johnson, Harold I., and Brown, B. Porter: Measurements of Aerodynamic Characteristics of a 35° Sweptback NACA 65-009 Airfoil Model with $\frac{1}{4}$-Chord Beveled-Trailing-Edge Flap and Trim Tab by the NACA Wing-Flow Method. NACA RM L9K11, 1950.
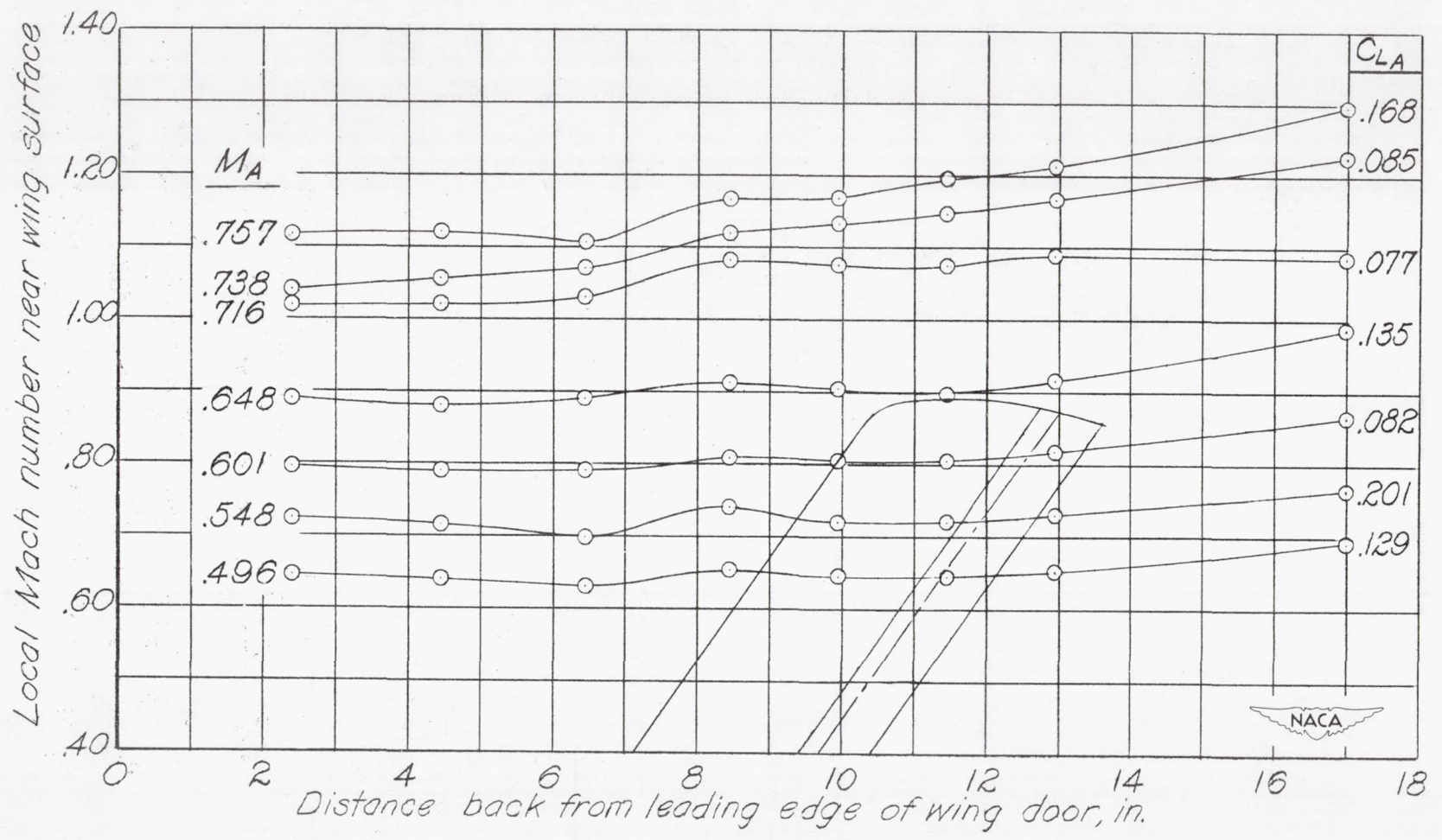
Figure 1.- Typical variations of local Mach number near wing surface with chordwise distance along wing surface for various airplane Mach numbers and lift coefficients as measured with model removed. Model location indicated by sketch.
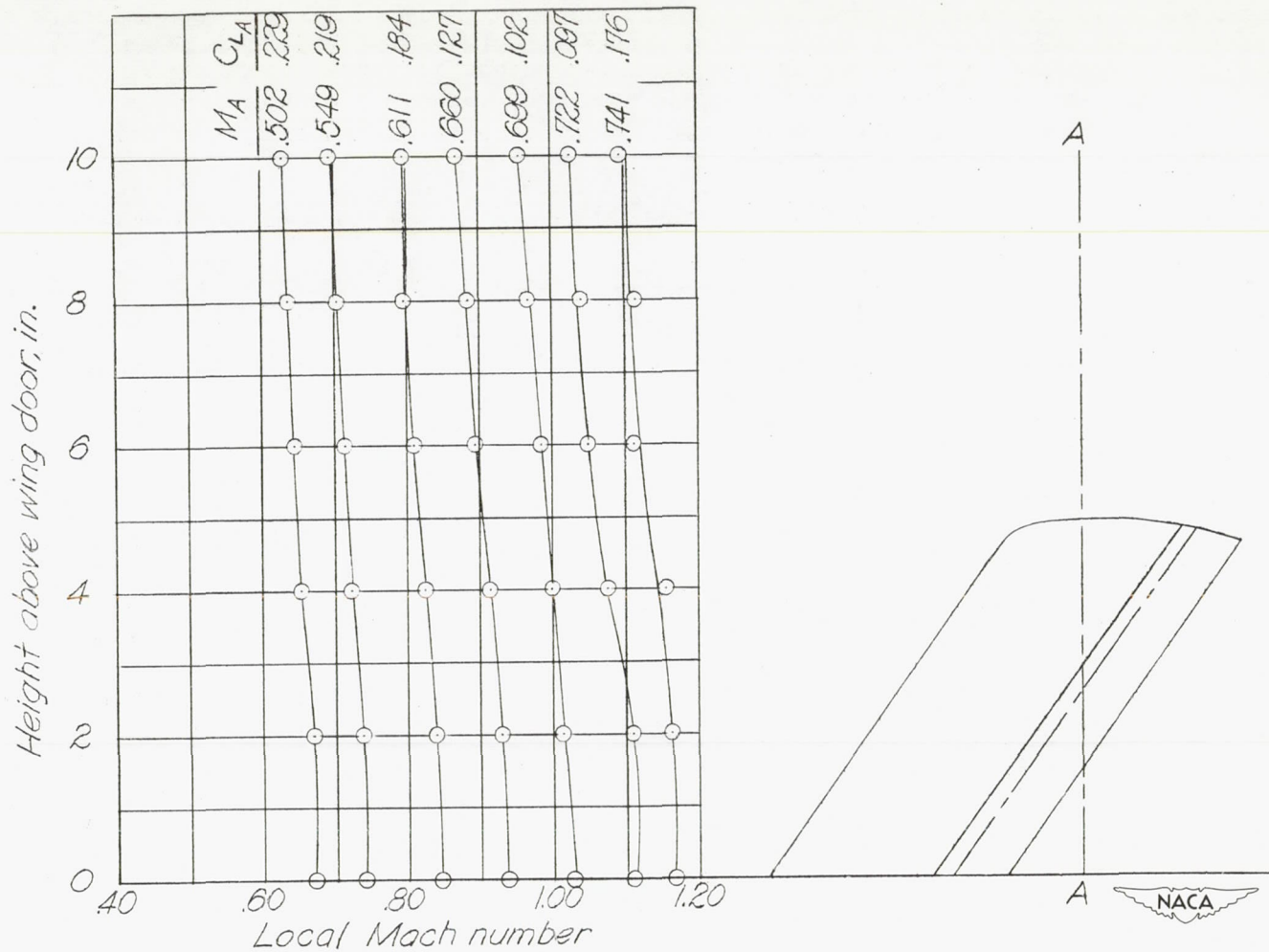
Figure 2.- Typical variations of local Mach number with vertical distance
above wing surface as measured at chordwise station AA with model
removed. Measurements made on left wing which had same contour as
right wing. No allowance made for wing boundary layer.

Figure 3.- Photograph of 35° sweptback NACA 65-009 model with $\frac{1}{4}$ - chord overhang-balanced flap.
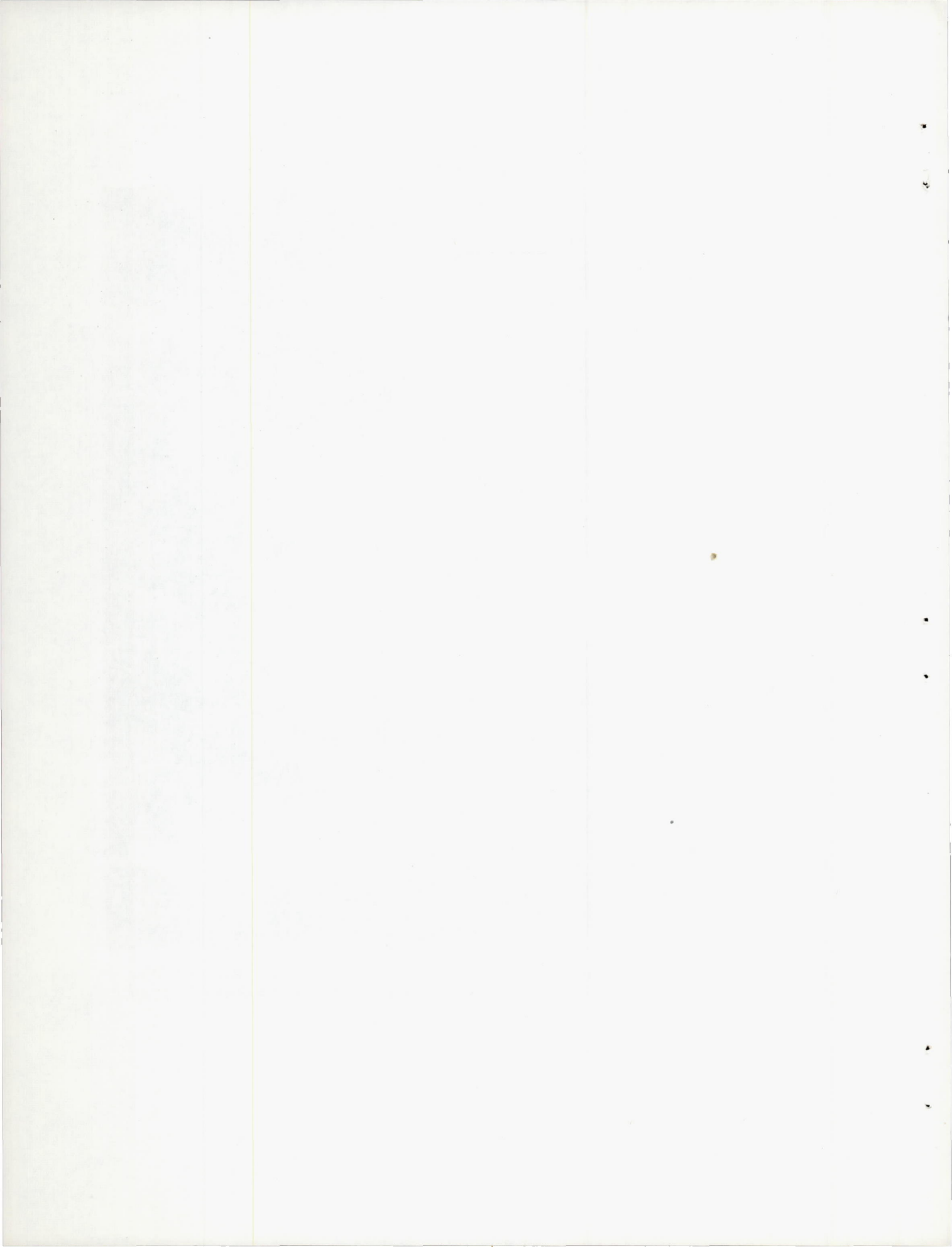
$\Lambda = 35^\circ$ $c_f = 0.25c$

$\lambda = 1.0$ $\overline{c}_f = 0.655$ in.

$A = 3.06$ $S_f = 3.78$ sq. in.

$b = 4.89$ in. $\phi = 6.0^\circ$

$\overline{c} = 3.25$ in. $c_b = 0.205$ in.

$S = 15.65$ sq. in. $c_b = 0.31\overline{c}_f$

$b_f = 5.88$ in.

2.655"

2.00"

.205"

.655"

5.97"

4.89"

M.A.C. = 3.25"

2.44"

35°

A

A

5.88"

SECTION AA
NACA 65-009
DOUBLE SIZE

≈.013" GAP

WING SURFACE

.75c   .25c

3.25"
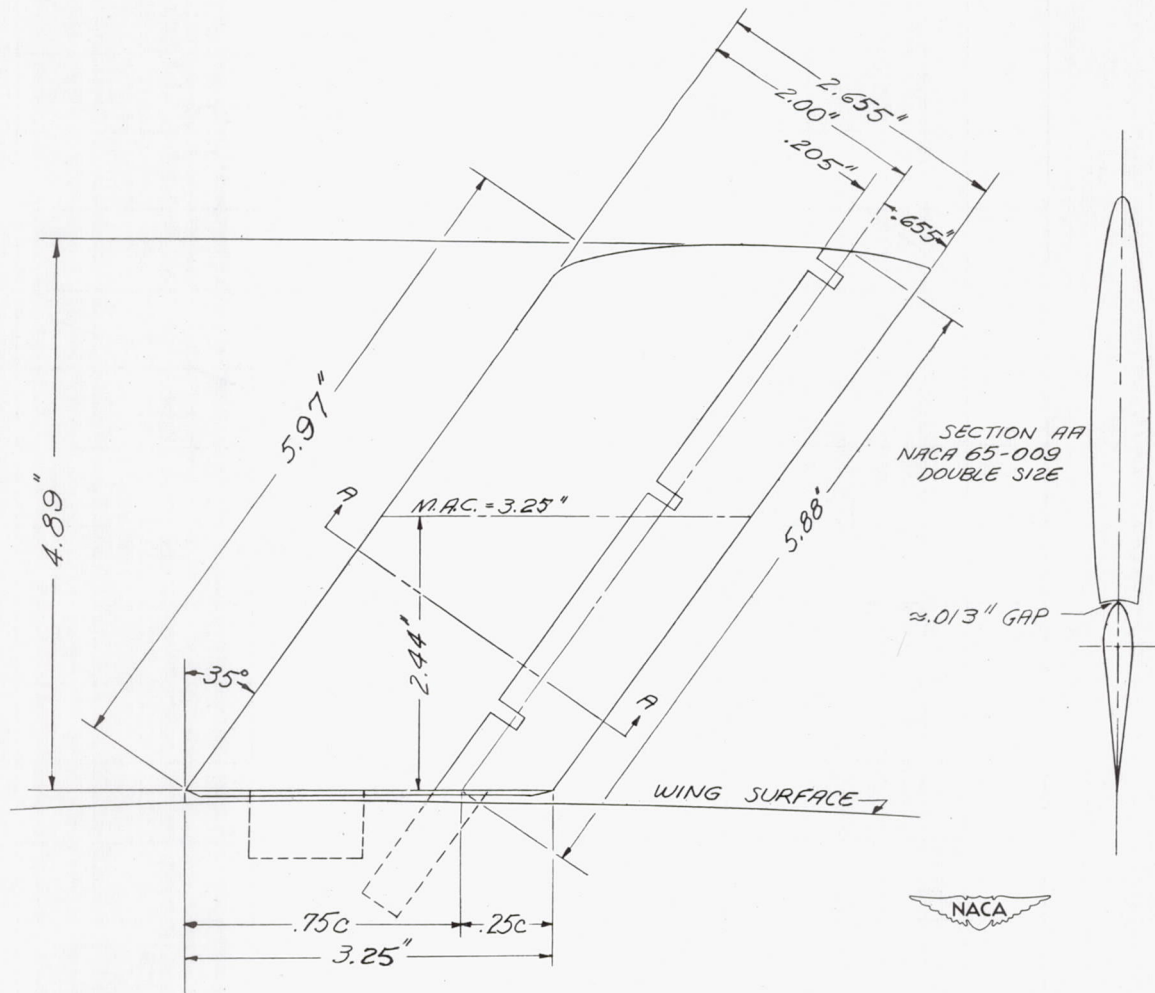
NACA

Figure 4.- Plan form and cross section of 35° sweptback NACA 65-009
airfoil with 25-percent-chord, full-span, overhang-balanced flap.
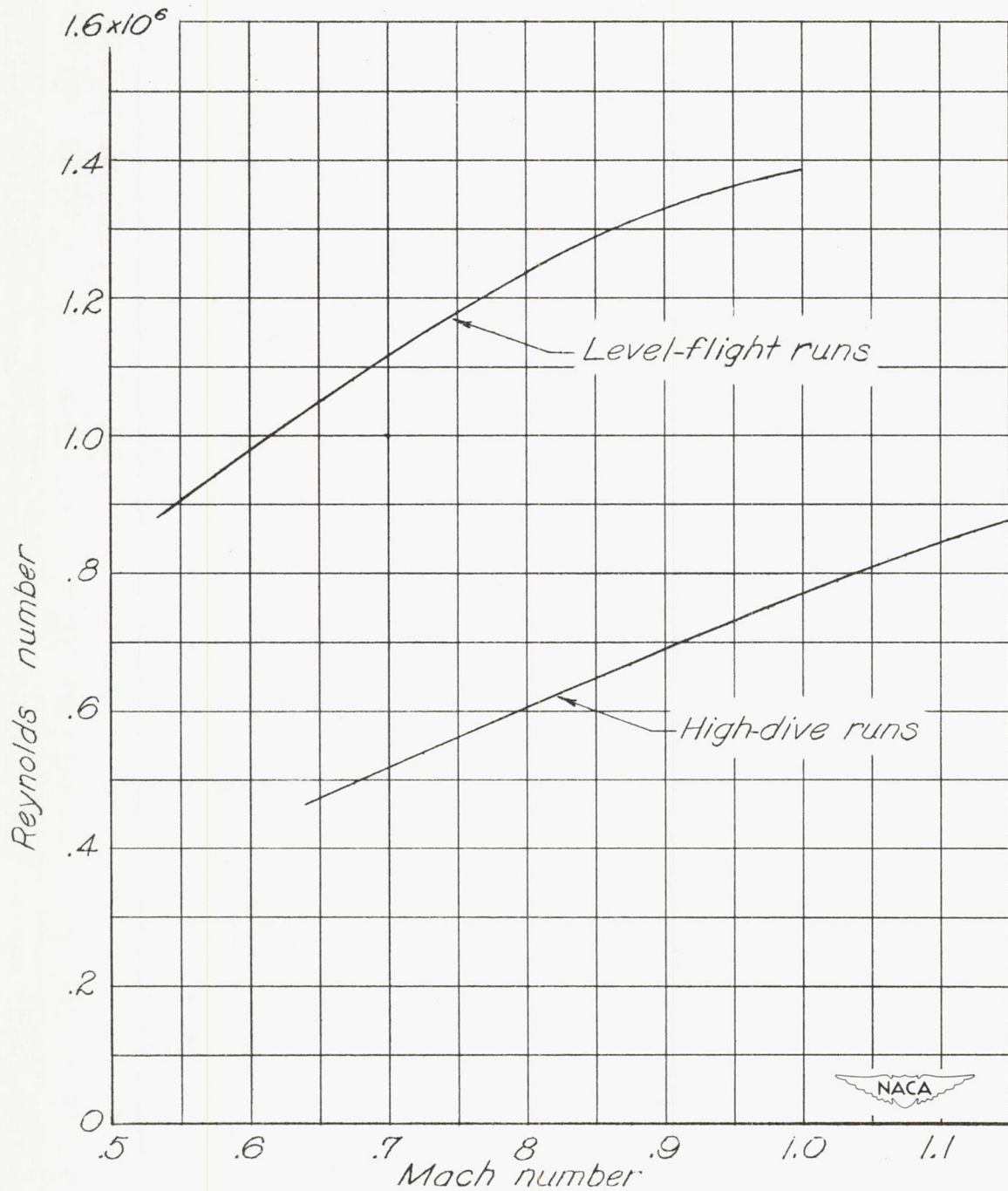
Figure 5.- Variation of Reynolds number with Mach number for tests of $35°$ sweptback, NACA 65-009 airfoil model with $\frac{1}{4}$ - chord overhang-balanced flap by the wing-flow method. Reynolds number based on airfoil chord parallel to direction of flow.
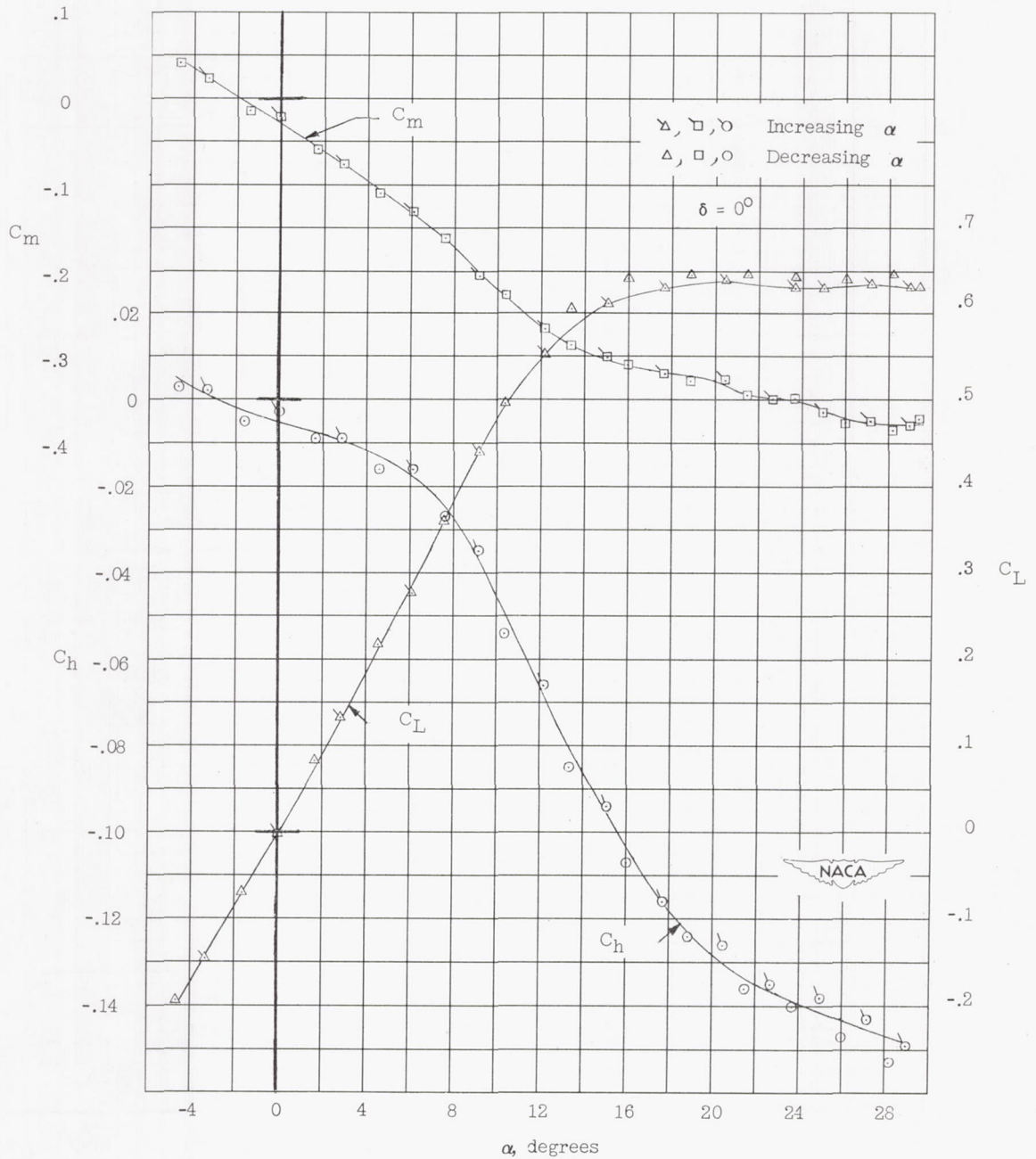
(a) Variation of C_L, C_m, and C_h with angle of attack.

Figure 6.- Typical examples of basic data obtained from strain-gage
   balance. NACA 65-009 airfoil, A = 3.06, c_f = 0.25c, overhang-
   balanced flap. Level-flight run, M = 0.75.
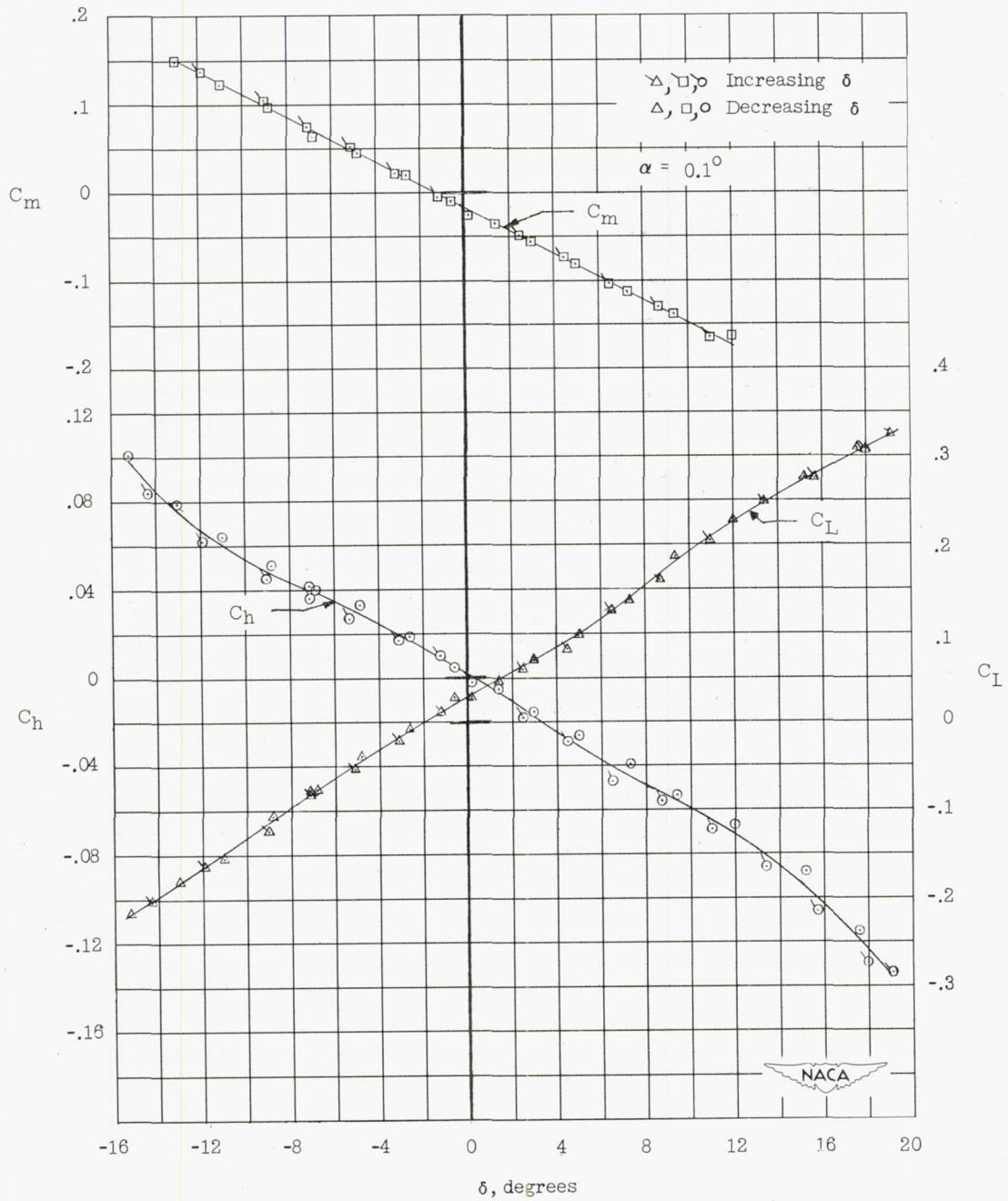
(b) Variation of C_L, C_m, and C_h with flap deflection.

Figure 6.- Concluded.
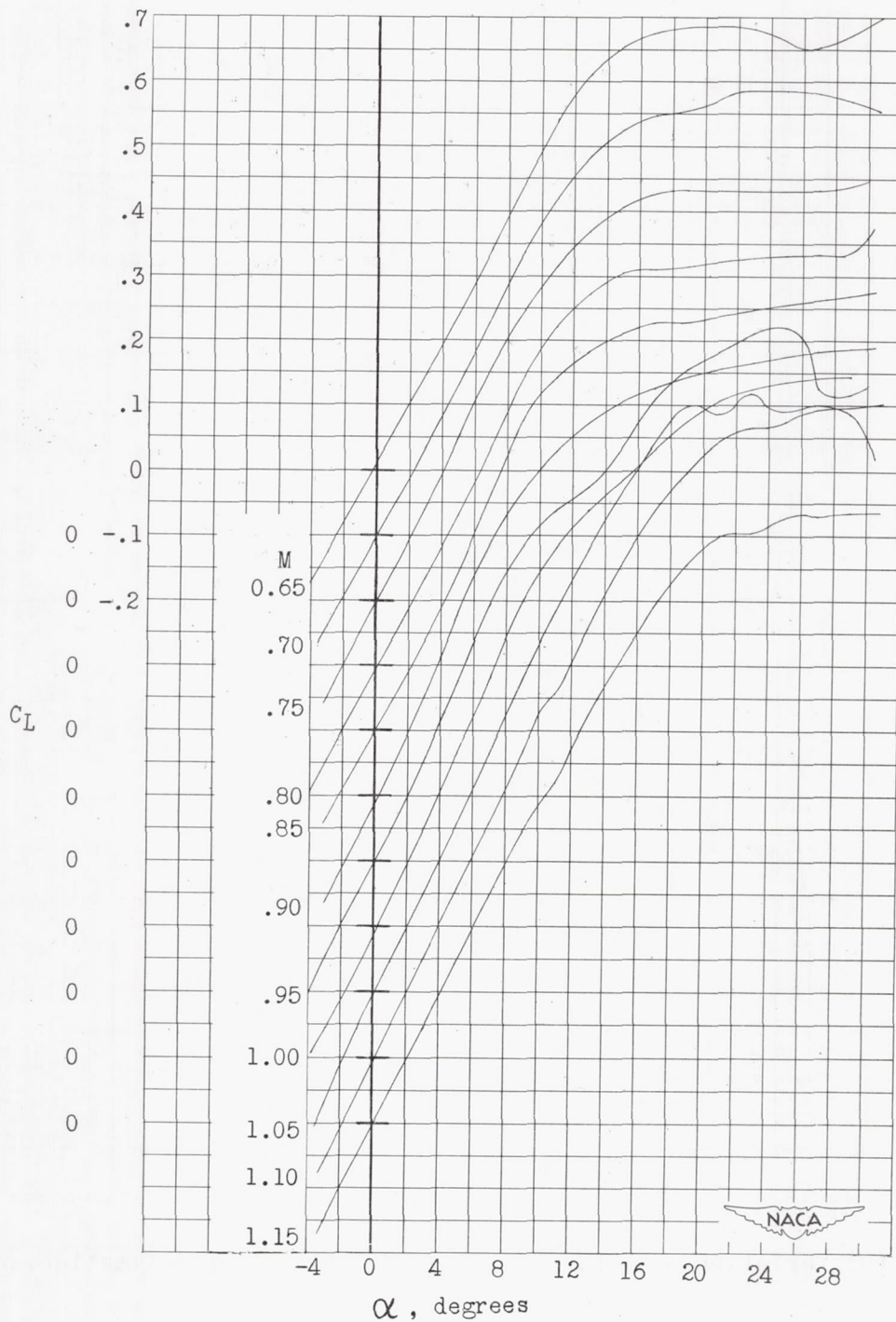
(a) High-dive runs.

Figure 7.- Variation of lift coefficient with angle of attack throughout
Mach number range for δ = 0°. NACA 65-009 airfoil, A = 3.06,
Λ = 35°, c_f = 0.25c, overhang-balanced flap.

α, degrees
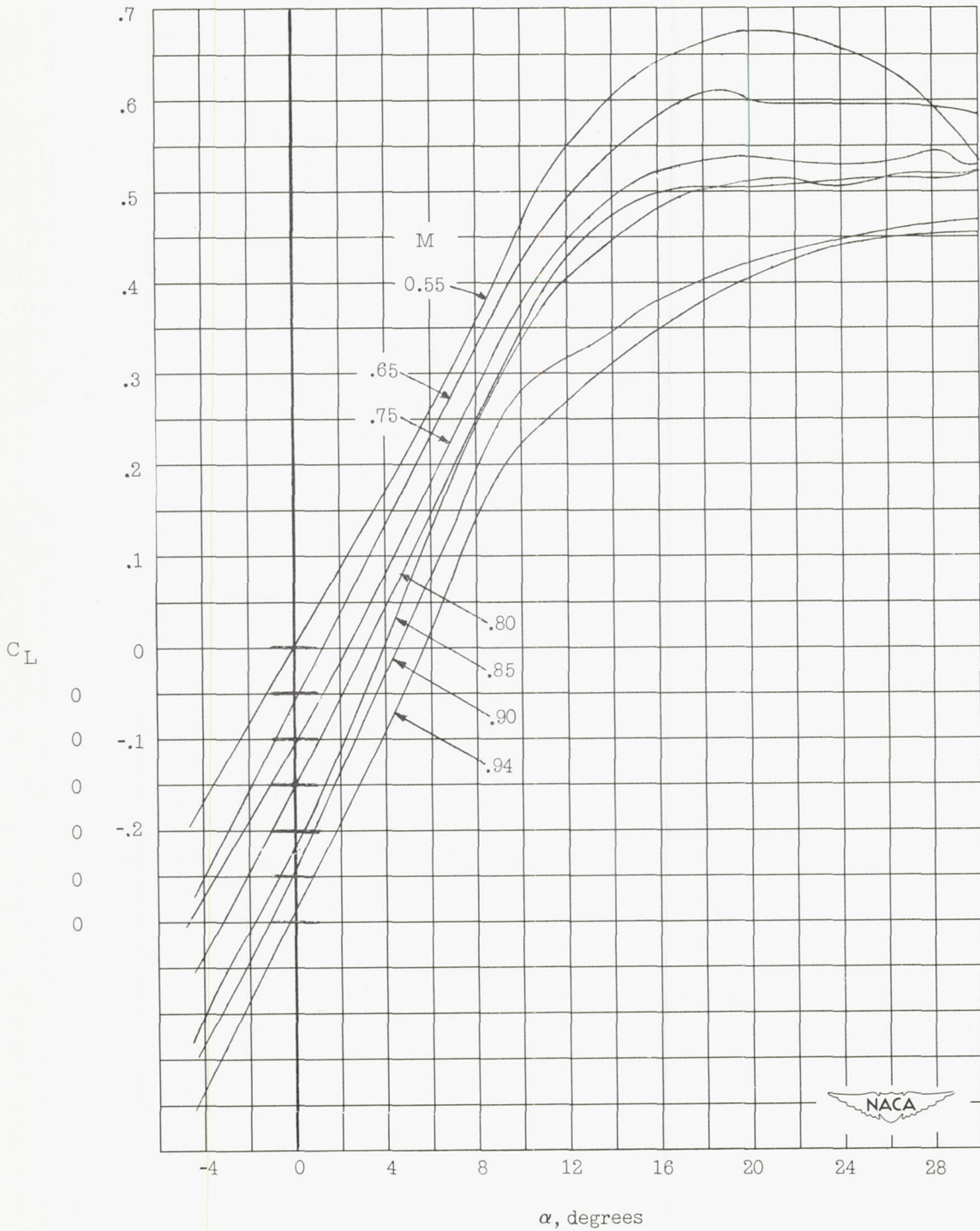
(b) Level-flight runs.

Figure 7.- Concluded.
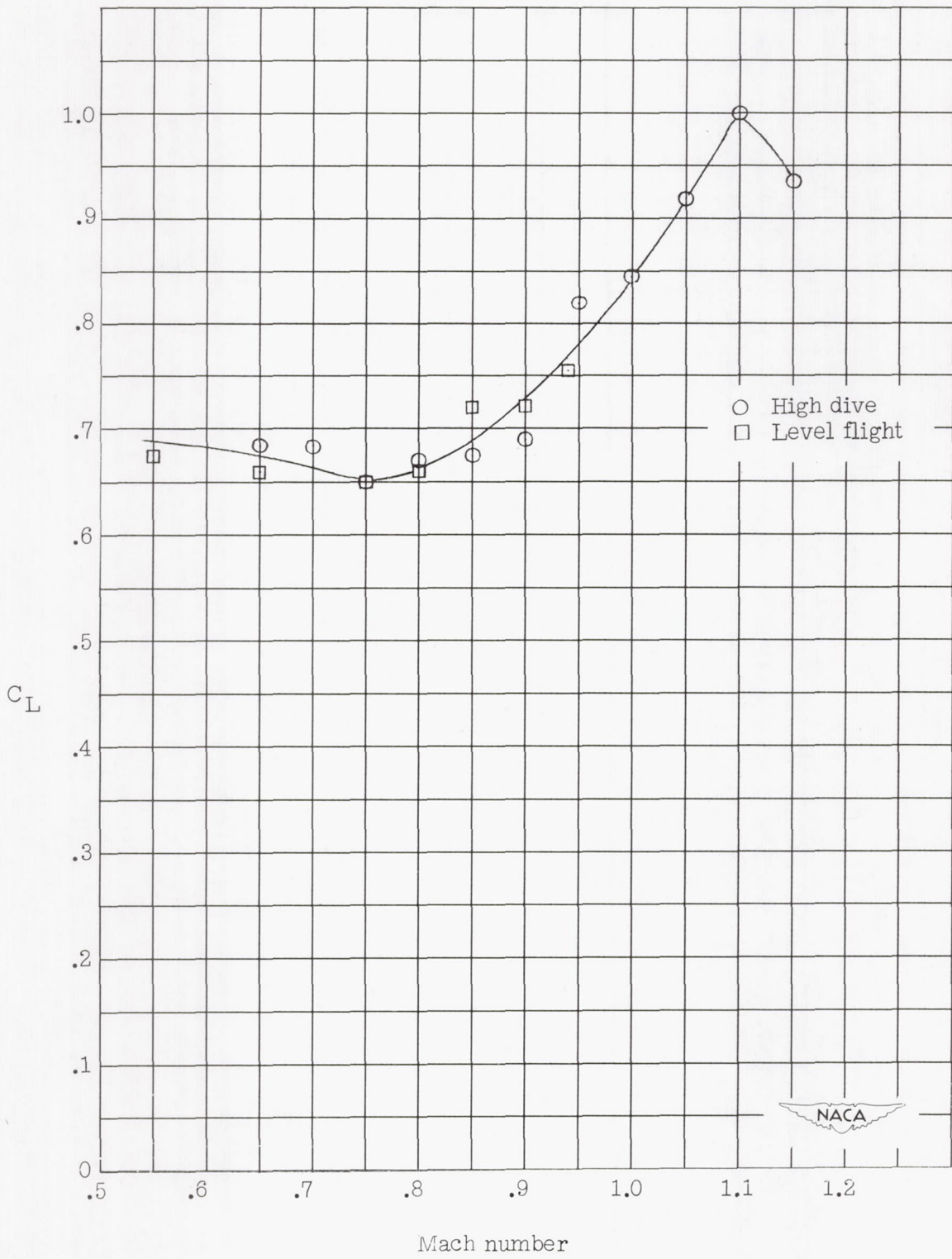
Figure 8.- Variation of maximum lift coefficient obtained below $\alpha \approx 30^{\circ}$ with Mach number.
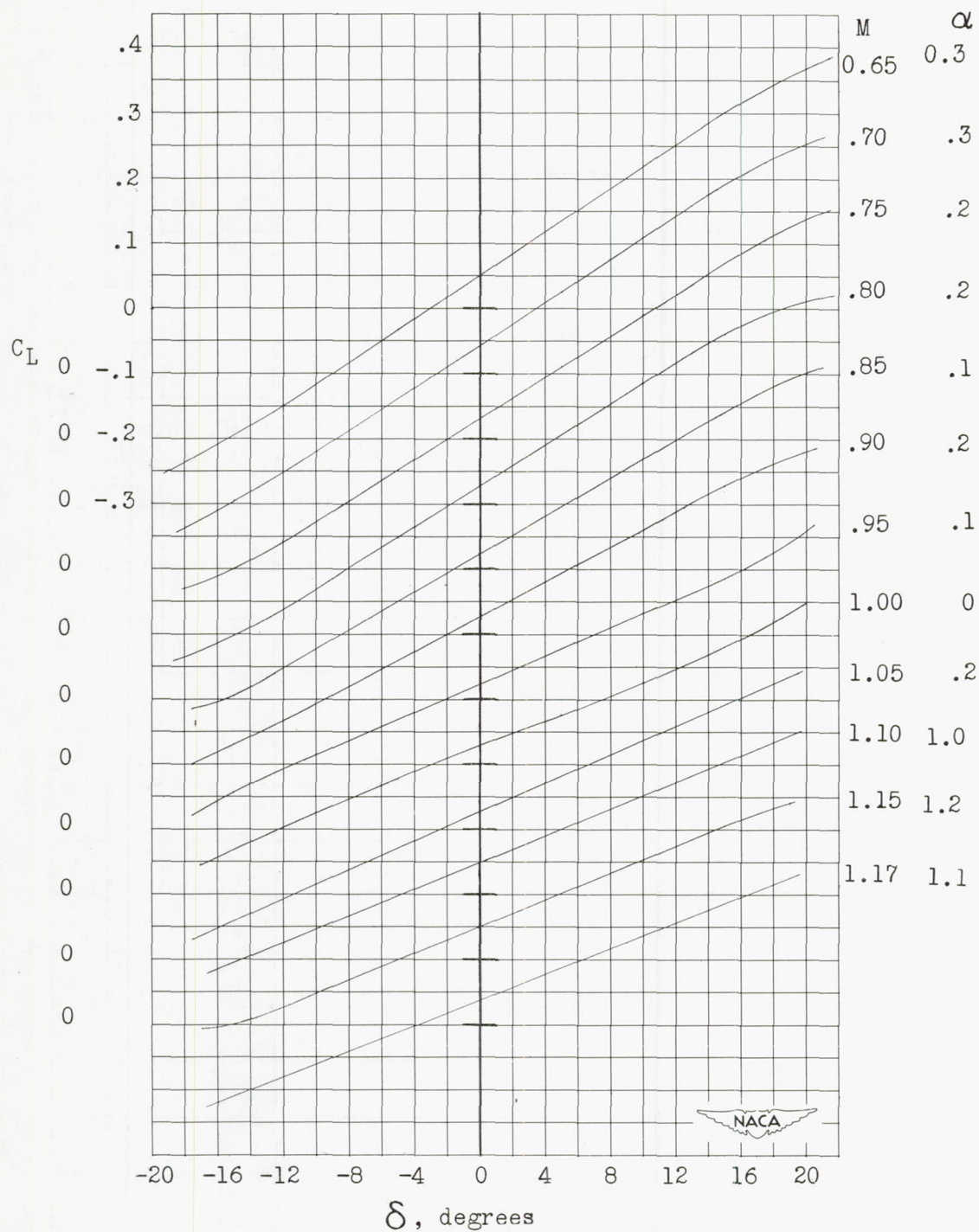
(a) High-dive runs.

Figure 9.- Variation of lift coefficient with flap deflection throughout
Mach number range for $\alpha \approx 0^\circ$. NACA 65-009 airfoil, A = 3.06,
$\Lambda = 35^\circ$, $c_f = 0.25c$, overhang-balanced flap.
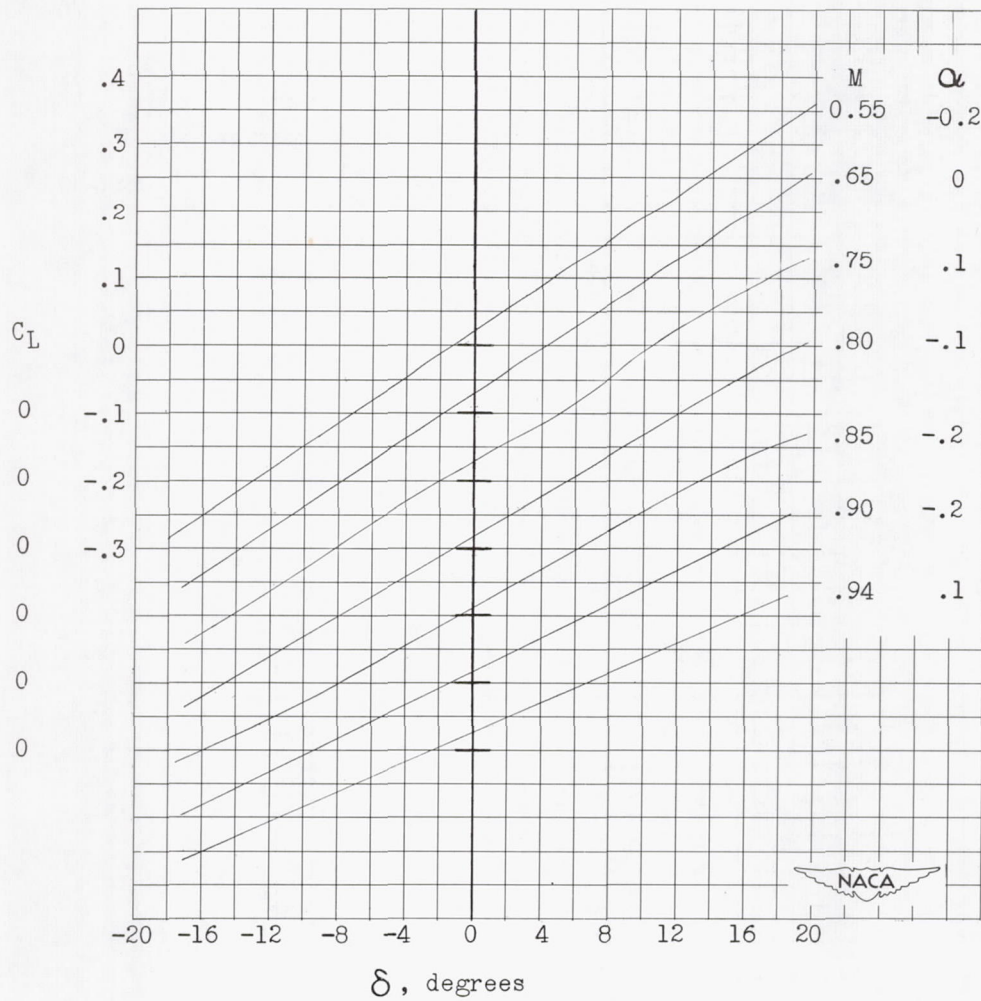
(b) Level-flight runs.

Figure 9.- Concluded.
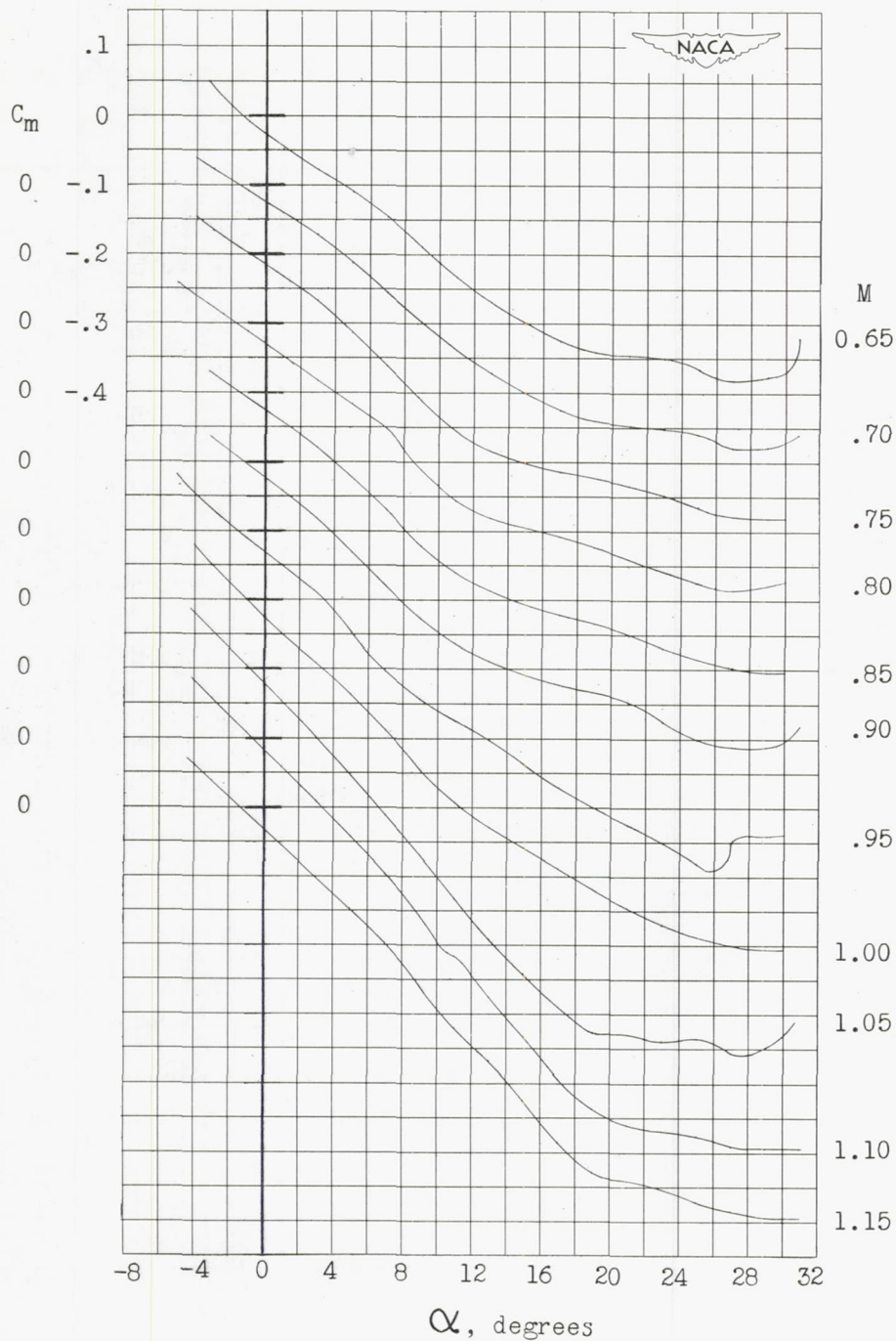
(a) High-dive runs.

Figure 10.- Variation of pitching-moment coefficient with angle of
attack throughout Mach number range for δ = 0°. NACA 65-009 airfoil,
A = 3.06, Λ = 35°, c_f = 0.25c, overhang-balanced flap. Moment
coefficient given about axis located 17.8 percent mean aerodynamic
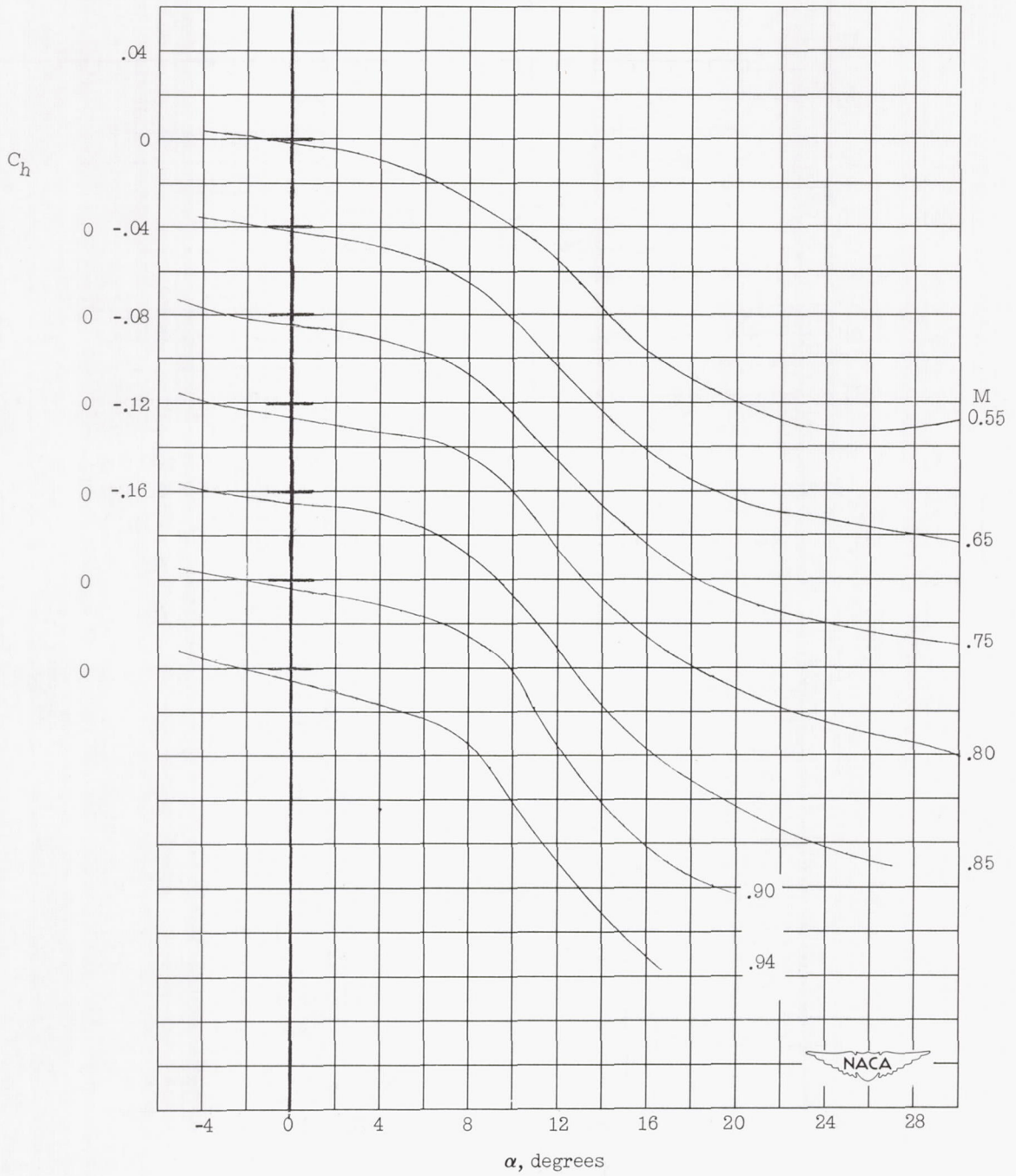chord ahead of leading edge of mean aerodynamic chord.
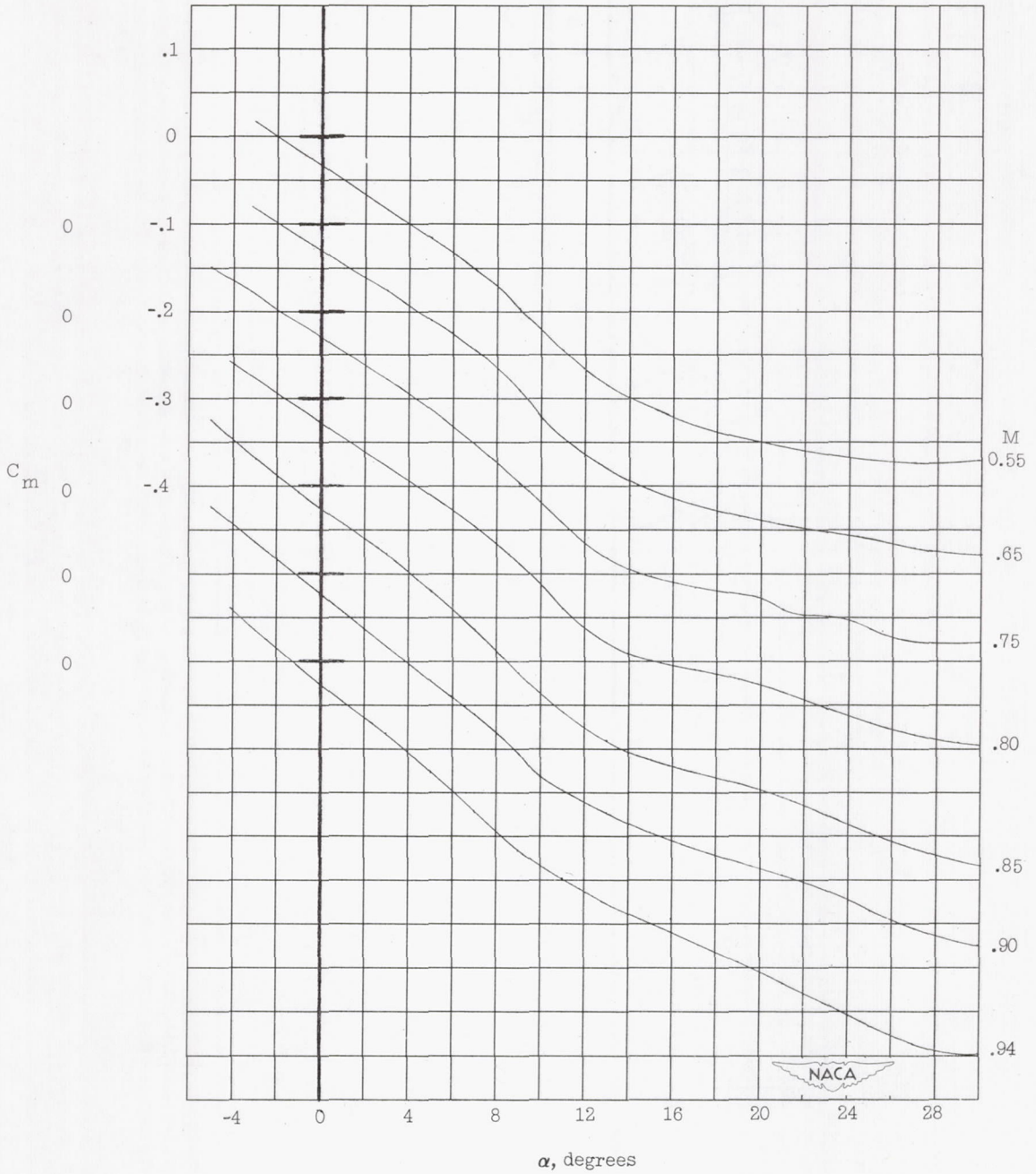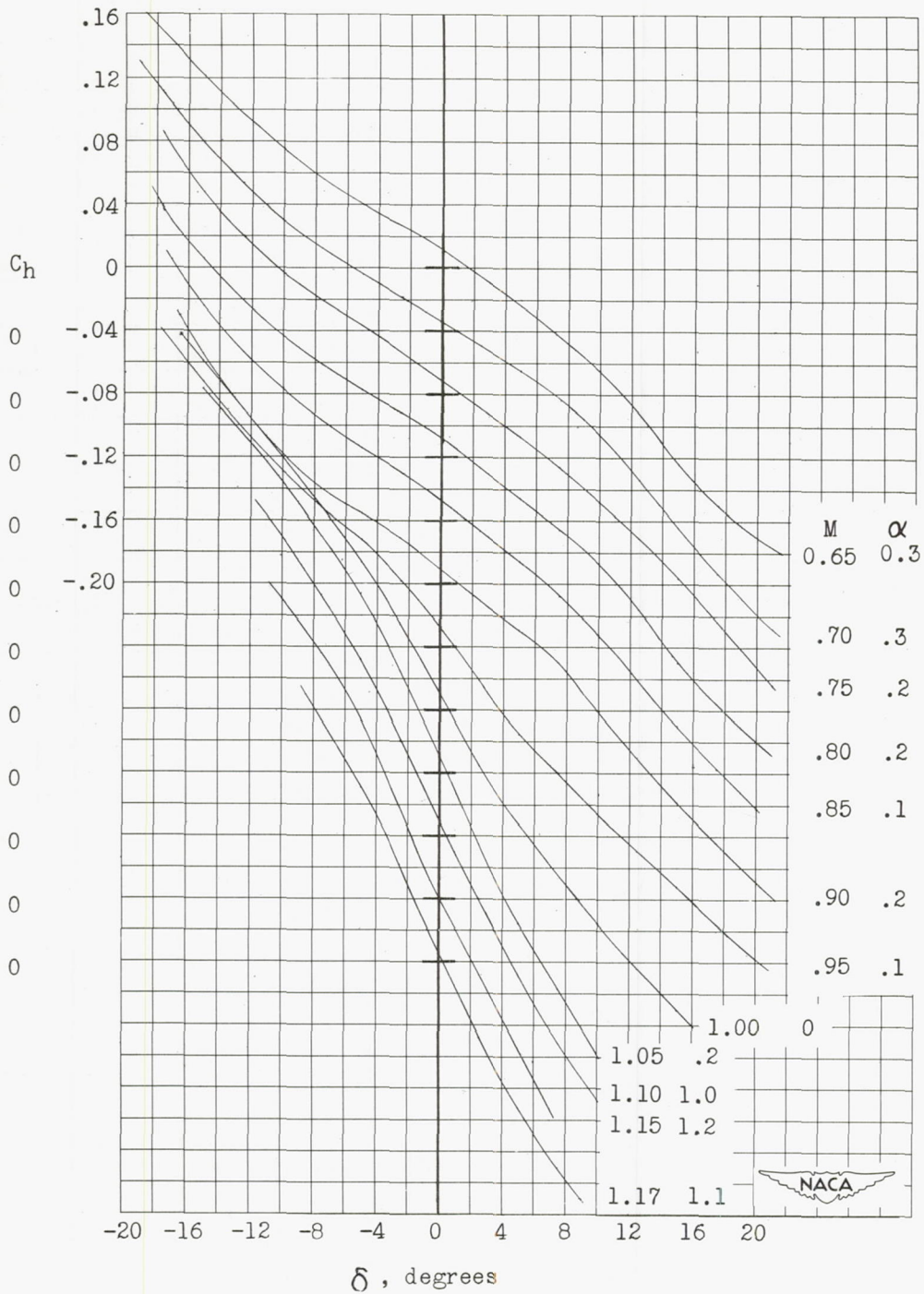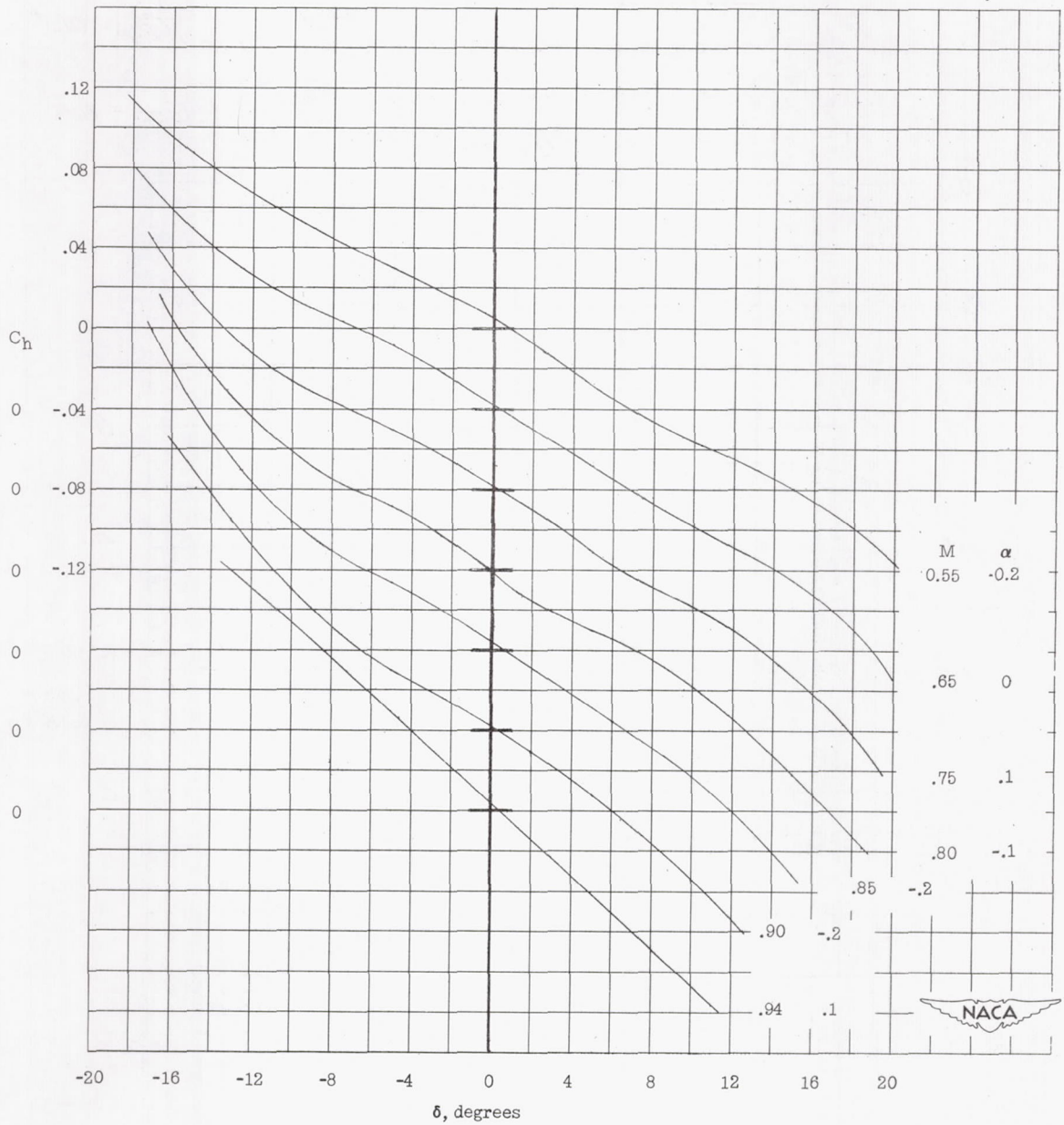
(b) Level-flight runs.

Figure 10.- Concluded.
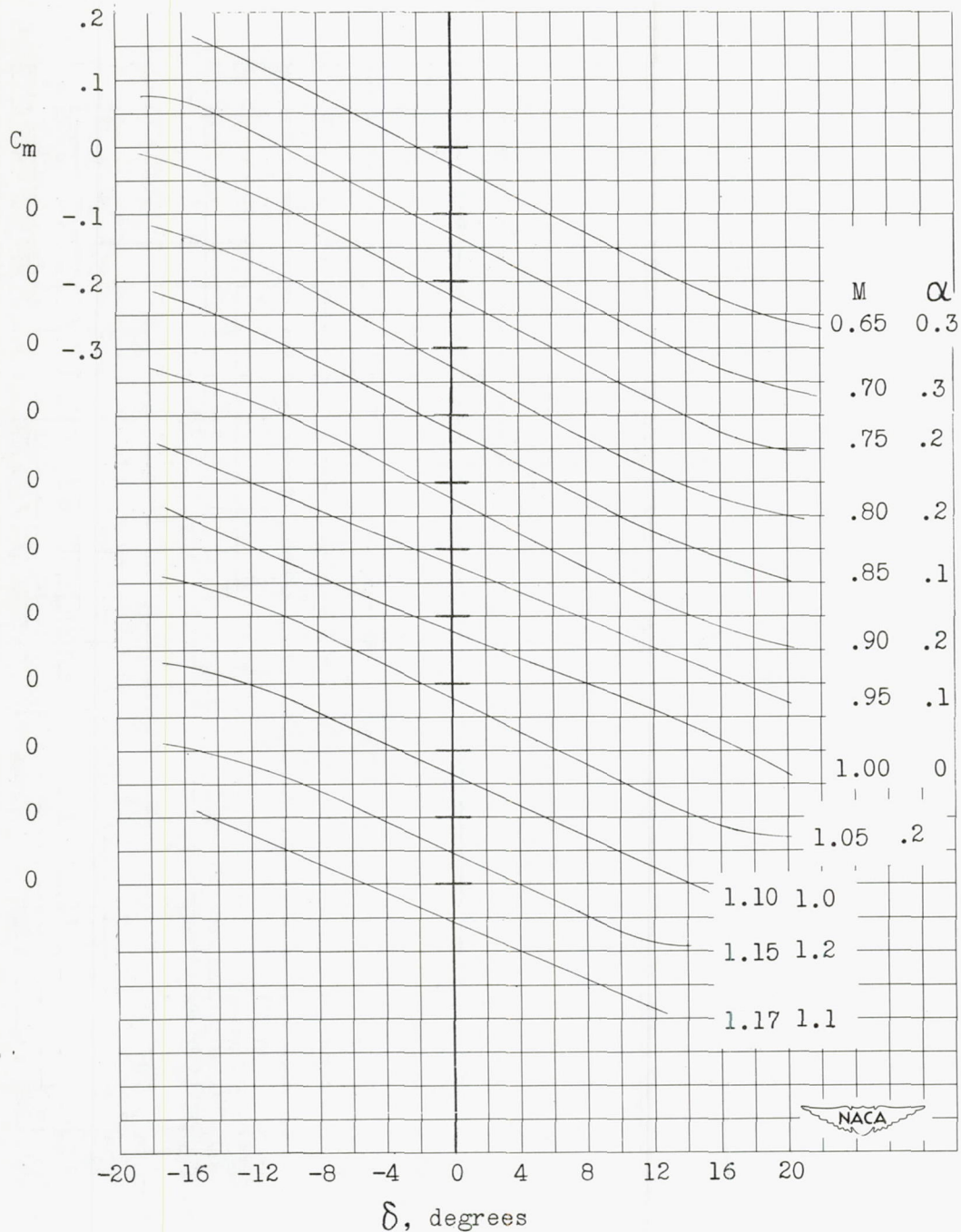
(a) High-dive runs.

Figure 11.- Variation of pitching-moment coefficient with flap deflection
   throughout Mach number range for $\alpha \approx 0^{\circ}$. NACA 65-009 airfoil,
   A = 3.06, $\Lambda = 35^{\circ}$, $c_f = 0.25c$, overhang-balanced flap. Moment
   coefficient given about axis located 17.8 percent mean aerodynamic
   chord ahead of leading edge of mean aerodynamic chord.

C_m

M   α
0.55   -0.2

.65   0

.75   .1

.80   -.1

.85   -.2

.90   -.2

.94   .1

-16   -12   -8   -4   0   4   8   12   16   20

δ , degrees
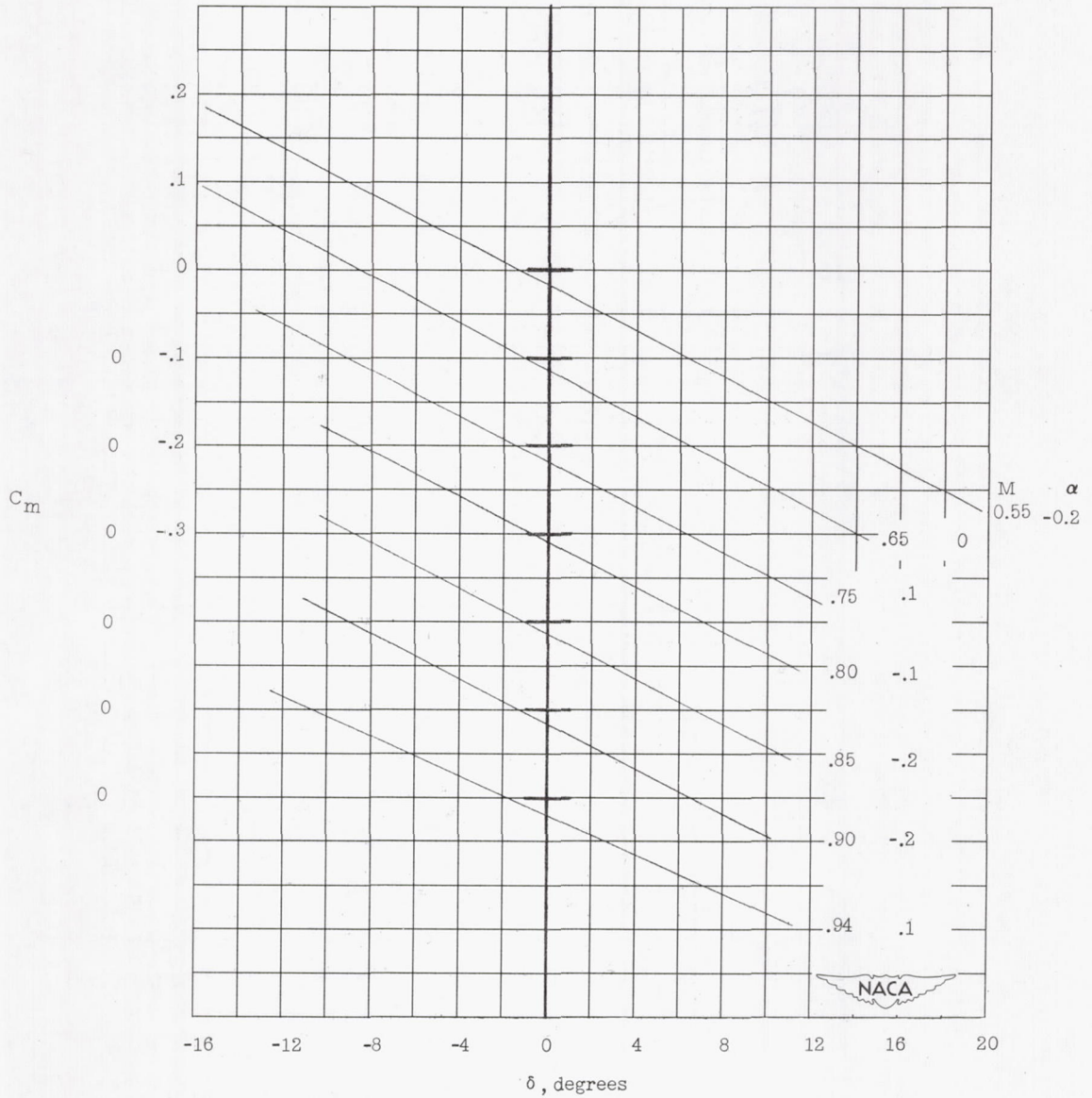
(b) Level-flight runs.

Figure 11.- Concluded.
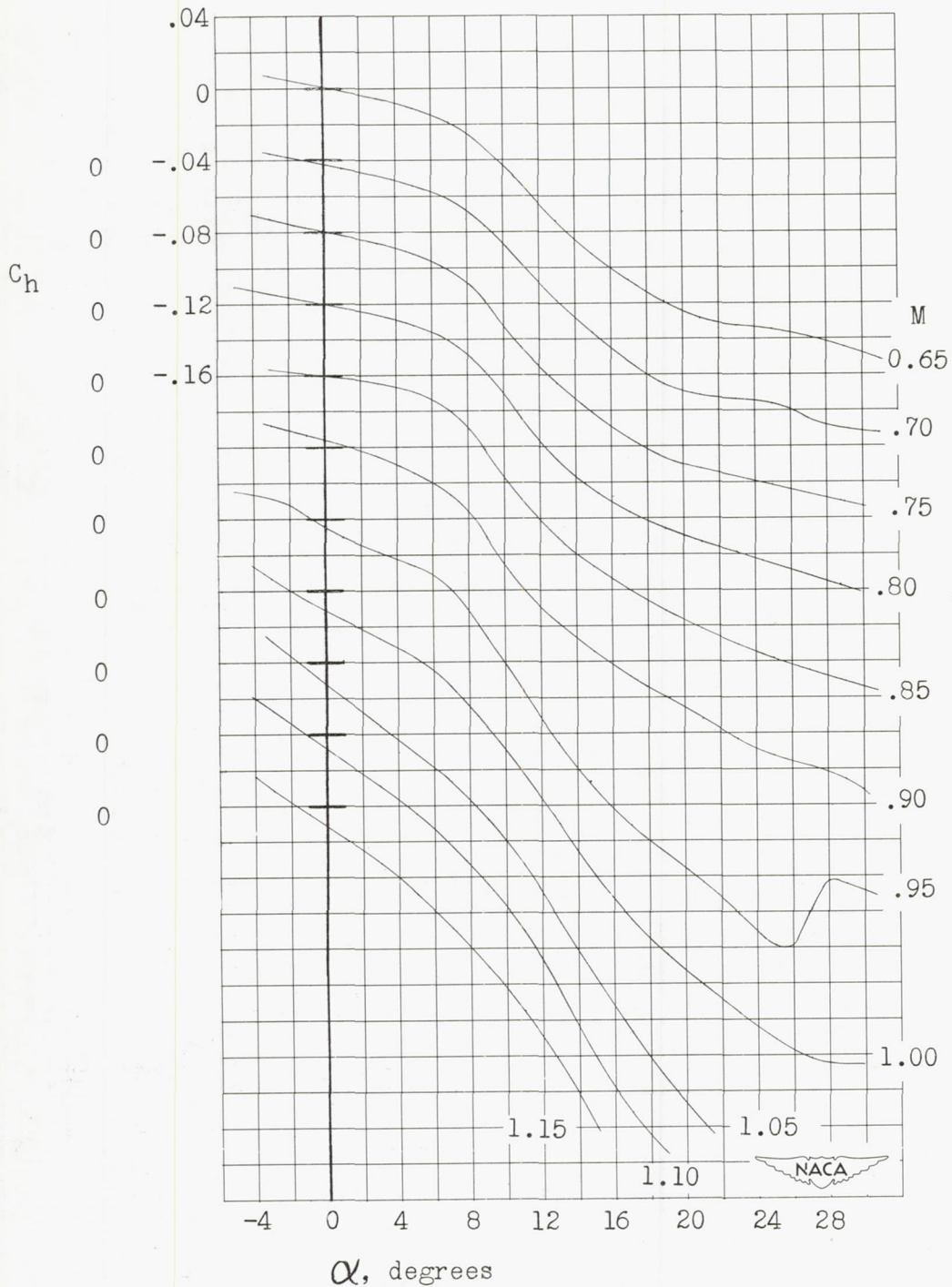
(a) High-dive runs.

Figure 12.- Variation of hinge-moment coefficient with angle of attack throughout Mach number range for $\delta = 0°$. NACA 65-009 airfoil, $A = 3.06$, $\Lambda = 35°$, $c_f = 0.25c$, overhang-balanced flap.

(b) Level-flight runs.

Figure 12.- Concluded.

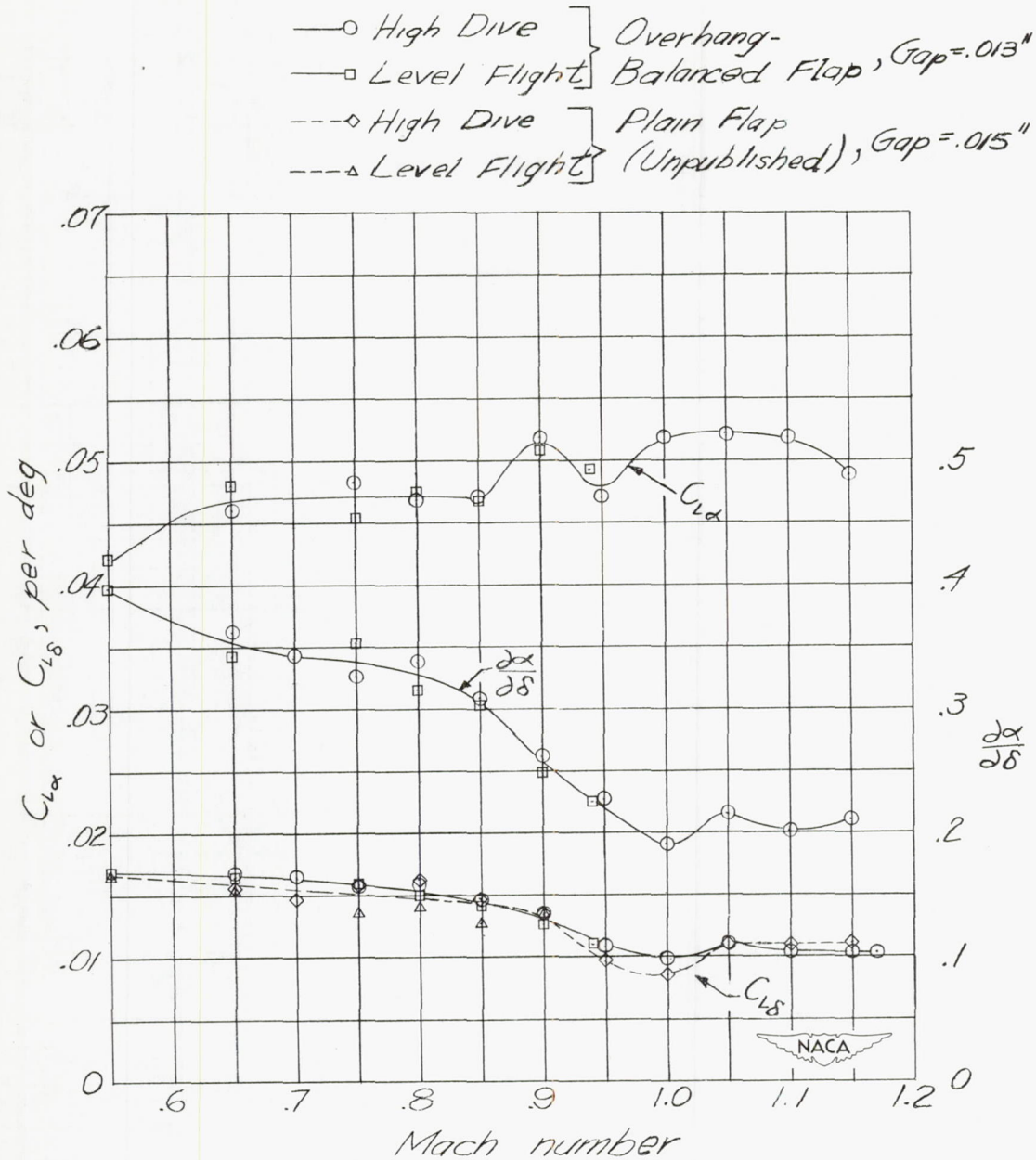(a) High-dive runs.

Figure 13.- Variation of hinge-moment coefficient with flap deflection
throughout Mach number range for α ≈ 0°. NACA 65-009 airfoil,
A = 3.06,   Λ = 35°, c_f = 0.25c,   overhang-balanced flap.

(b) Level-flight runs.

Figure 13.- Concluded.

Figure 14.- Variation of airfoil-model and flap lift effectiveness with
    Mach number for α ≈ 0°, δ$_f$ = 0°. NACA 65-009 airfoil, A = 3.06,
    Λ = 35°, c$_f$ = 0.25c, overhang-balanced flap.

Figure 15.- Variation of airfoil-model and flap pitching-moment charac-
teristics with Mach number for $\alpha \approx 0°$, $\delta_f = 0°$. NACA 65-009 airfoil,
A = 3.06, Λ = 35°, c_f = 0.25c, overhang-balanced flap. Pitching
moments measured about axis located 17.8 percent mean aerodynamic
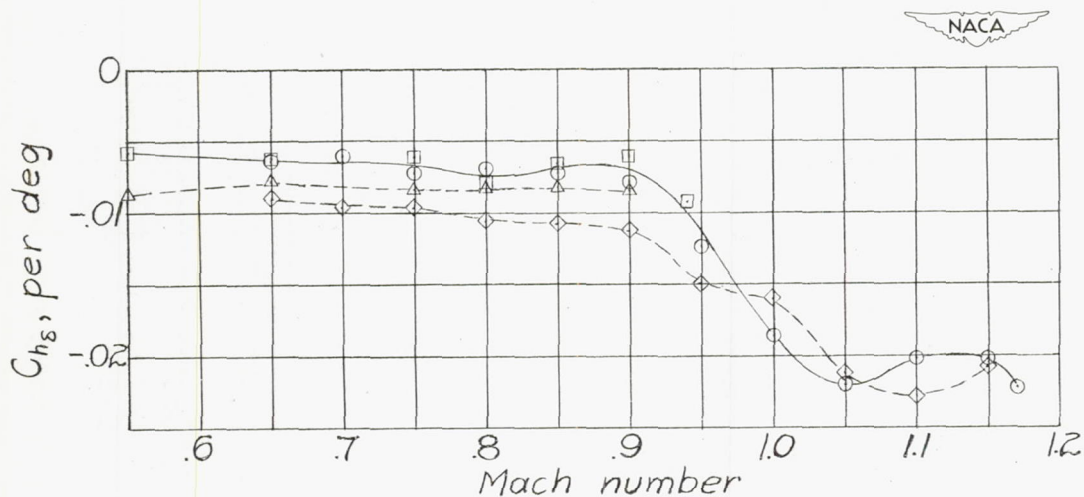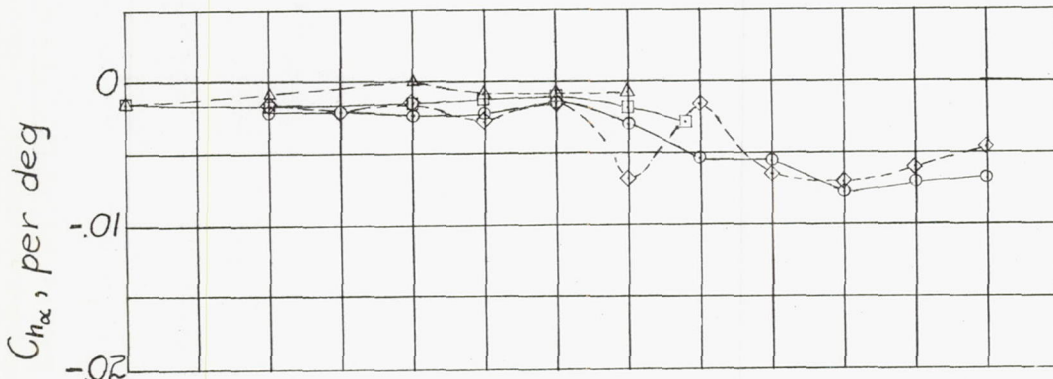chord ahead of leading edge of mean aerodynamic chord.

Figure 16.- Variation with Mach number of rate of change of hinge-moment
    coefficient with angle of attack and with flap deflection measured at
    $\alpha \approx 0^\circ$, $\delta_f = 0^\circ$. NACA 65-009 airfoil, $A = 3.06$, $\Lambda = 35^\circ$,
    $c_f = 0.25c$, overhang-balanced flap.